Molecular Biology of the Cell
Vol. 10, 3015–3033, September 1999

A Role for the GSG Domain in Localizing Sam68 to Novel Nuclear Structures in Cancer Cell Lines

Taiping Chen,* François-Michel Boisvert,† David P. Bazett-Jones,† and Stéphane Richard*‡

*Terry Fox Molecular Oncology Group, Lady Davis Institute for Medical Research, Sir Mortimer B. Davis Jewish General Hospital, and Departments of Oncology, Medicine, and Microbiology and Immunology, McGill University, Montréal, Québec H3T 1E2, Canada; and †Department of Cell Biology and Anatomy, University of Calgary, Calgary, Alberta T2N 4N1, Canada

Submitted April 8, 1999; Accepted June 24, 1999
Monitoring Editor: Joseph Gall

The GSG (GRP33, Sam68, GLD-1) domain is a protein module found in an expanding family of RNA-binding proteins. The numerous missense mutations identified genetically in the GSG domain support its physiological role. Although the exact function of the GSG domain is not known, it has been shown to be required for RNA binding and oligomerization. Here it is shown that the Sam68 GSG domain plays a role in protein localization. We show that Sam68 concentrates into novel nuclear structures that are predominantly found in transformed cells. These Sam68 nuclear bodies (SNBs) are distinct from coiled bodies, gems, and promyelocytic nuclear bodies. Electron microscopic studies show that SNBs are distinct structures that are enriched in phosphorus and nitrogen, indicating the presence of nucleic acids. A GFP-Sam68 fusion protein had a similar localization as endogenous Sam68 in HeLa cells, diffusely nuclear with two to five SNBs. Two other GSG proteins, the Sam68-like mammalian proteins SLM-1 and SLM-2, colocalized with endogenous Sam68 in SNBs. Different GSG domain missense mutations were investigated for Sam68 protein localization. Six separate classes of cellular patterns were obtained, including exclusive SNB localization and association with microtubules. These findings demonstrate that the GSG domain is involved in protein localization and define a new compartment for Sam68, SLM-1, and SLM-2 in cancer cell lines.

INTRODUCTION

The GSG (GRP33, Sam68, GLD-1) domain is an ~200-amino acid protein module found in proteins closely associated with RNA (Jones and Schedl, 1995). GSG domain–containing proteins include the *Artemia salina* GRP33 (Cruz-Alvarez and Pellicer, 1987), mammalian Sam68 (Wong *et al.*, 1992), *Caenorhabditis elegans* GLD-1 (Jones and Schedl, 1995), SF1 (Arning *et al.*, 1996), *Drosophila* Who/How (Baehrecke, 1997; Fyrberg *et al.*, 1997; Zaffran *et al.*, 1997), *Xenopus* Xqua (Zorn *et al.*, 1997), mouse Qk1 (Ebersole *et al.*, 1996), zebrafish Qk1 (Tanaka *et al.*, 1997), mouse SLM-1 and SLM-2 (Di Fruscio *et al.*, 1999), *Drosophila* KEP1 and Sam50 (Di Fruscio *et al.*, 1998), and *Drosophila* Qk1-related proteins (Fyrberg *et al.*, 1998). The GSG domain is also called STAR, for signal transduction and activation of RNA, domain (Vernet and Artzt, 1997). In the GSG domain is embedded an extended heterogeneous nuclear ribonucleoprotein (hnRNP) K homology (KH) domain that contains 6 and 20 extra amino acids in KH domain loops 1 and 4, respectively (Gibson *et al.*, 1993). Although the roles of these extended KH domain loops are unknown, they have been postulated to mediate protein-protein interactions (Musco *et al.*, 1996). Indeed, we have shown that the KH domain loops 1 and 4 are required for Sam68 multimerization (Chen *et al.*, 1997). Although the exact function of the GSG domain is unknown, two properties have been ascribed to this protein module: self-association (Chen *et al.*, 1997; Zorn and Krieg, 1997; Di Fruscio *et al.*, 1998) and RNA binding (Berglund *et al.*, 1997; Chen *et al.*, 1997; Lin *et al.*, 1997; Zorn and Krieg, 1997; Chen and Richard, 1998; Di Fruscio *et al.*, 1998, 1999; Rain *et al.*, 1998).

Genetic mutations in the GSG domain that result in growth or developmental defects have been isolated in a number of genes, supporting a physiological role for this protein module. In *C. elegans*, the GSG protein GLD-1 is required for normal oocyte development and has been

‡ Corresponding author. E-mail address: mcrd@musica.mcgill.ca.
Abbreviations used: BrdU, bromodeoxyuridine; Br-UTP, bromouridine triphosphate; GFP, green fluorescent protein; GSG domain, GRP33, Sam68, GLD-1 domain; KH, hnRNP K homology; NLS, nuclear localization signal; PNC, perinucleolar compartment; PTB, polypyrimidine tract–binding protein; SNBs, Sam68 nuclear bodies.

shown to function as a tumor suppressor (Francis *et al.*, 1995a,b). Thirty-two *gld-1* mutations, including several missense mutations within the GSG domain, have been identified and classified into six phenotypic classes (Jones and Schedl, 1995). In mice, the GSG protein Qk1 is involved in myelination and early embryogenesis (Hogan and Greenfield, 1984). A missense mutation (E48G) identified in the N-terminal portion of the Qk1 GSG domain is known to be embryonic lethal in mice (Justice and Bode, 1988; Ebersole *et al.*, 1996). The molecular defect is most likely due to the failure of the Qk1 proteins to dimerize (Chen and Richard, 1998). The *Drosophila melanogaster* GSG protein Who/How plays a critical role in skeletal muscle development, as weak alleles, including a missense mutation in KH domain loop 4, result in the "wings-held-out" phenotype (Baehrecke, 1997; Fyrberg *et al.*, 1997; Zaffran *et al.*, 1997).

The GSG protein Sam68 is a substrate for Src kinases during mitosis (Fumagalli *et al.*, 1994; Taylor and Shalloway, 1994), and it has been proposed to serve as an adapter protein for Src kinases (Richard *et al.*, 1995; Taylor *et al.*, 1995). Sam68 is an RNA-binding protein (Wong *et al.*, 1992), and its RNA-binding activity is negatively regulated by tyrosine phosphorylation (Wang *et al.*, 1995). The nuclear localization of Sam68 (Wong *et al.*, 1992; Ishidate *et al.*, 1997) suggests that it may interact with cytoplasmic proteins, including Src kinases, during mitosis, when the nuclear envelope breaks down. Two Sam68-like proteins, SLM-1 and SLM-2, were recently identified (Di Fruscio *et al.*, 1999). They are both nuclear proteins that heterodimerize with Sam68 (Di Fruscio *et al.*, 1999). SLM-1 is tyrosine phosphorylated by Src kinases during mitosis, like Sam68, whereas SLM-2 is not a substrate for Src kinases (Di Fruscio *et al.*, 1999). The functions of Sam68, SLM-1, and SLM-2 are currently unknown.

The nucleus contains a number of specialized subnuclear structures, including the nucleolus, interchromatin granule speckles, coiled bodies, gems, and promyelocytic (PML) nuclear bodies (Lamond and Earnshaw, 1998). Speckles are observed when immunostained with antibodies to splicing factors such as SC35 (Fu and Maniatis, 1990) and represent aggregates of snRNPs and splicing factors (Spector, 1993). Coiled bodies are round structures 0.1 to 1.0 μm in diameter containing coiled threads (Monneron and Bernhard, 1969). They contain spliceosomal small nuclear ribonucleoproteins (snRNPs), U3 small nucleolar ribonucleoprotein (snoRNP), fibrillarin, NOPP140, and an autoantigen called p80-coilin (Lamond and Carmo-Fonseca, 1993; Gall *et al.*, 1995). Antibodies against p80-coilin have been widely used as a marker for coiled bodies (Andrade *et al.*, 1993). Coiled bodies vary in number from 1 to 10, and the number increases markedly in cancer cells (Spector *et al.*, 1992). Gems (gemini of coiled bodies) are very similar to coiled bodies in number, size, and distribution pattern (Liu and Dreyfuss, 1996). However, gems and coiled bodies appear to be indistinguishable in some cell types (Matera and Frey, 1998; Bechade *et al.*, 1999). Gems contain the survival of motor neurons (SMN) protein (Liu and Dreyfuss, 1996), which is encoded by the gene responsible for spinal muscular atrophy (Lefebvre *et al.*, 1995), and an interacting protein, SIP1 (Liu *et al.*, 1997). SMN and SIP1 have been shown to interact with several spliceosomal snRNP proteins and play an essential role in snRNP biogenesis and pre-mRNA splicing (Fischer *et al.*, 1997; Liu *et al.*, 1997; Pellizzoni *et al.*, 1998). PML nuclear bodies, also known as PODs (PML oncogenic domain), are nuclear matrix-associated structures altered by oncoproteins and viruses (Dyck *et al.*, 1994; Weis *et al.*, 1994; Doucas *et al.*, 1996). Anti-PML antibodies serve as a marker for PML nuclear bodies. Generally, each mammalian cell contains 10–20 PML nuclear bodies, with sizes ranging from 0.3 to 1.0 μm. In acute promyelocytic leukemia cells, PML nuclear bodies are disorganized into micropunctate structures (Dyck *et al.*, 1994; Koken *et al.*, 1994; Weis *et al.*, 1994). The functions of coiled bodies, gems, and PML nuclear bodies remain unknown.

Here we demonstrate that Sam68, SLM-1, and SLM-2 are concentrated in distinct nuclear bodies. These nuclear structures show dynamic changes in response to transcriptional inhibitors and during mitosis. Sam68 nuclear bodies contain nucleic acids, as visualized by electron microscopy, but they are not the site of ongoing transcription, as determined by bromo (Br)-UTP incorporation. Double-immunostaining studies demonstrate that the Sam68 nuclear bodies are distinct from coiled bodies, gems, and PML nuclear bodies. Amino acid substitutions or deletions within the Sam68 GSG domain concentrate these mutant proteins in nuclear bodies, in the cytoplasm, and on microtubules. These data suggest that the GSG domain plays a role in localizing Sam68/SLM to different cellular compartments, including a novel nuclear structure.

MATERIALS AND METHODS

DNA Constructs

The green fluorescent protein (GFP)-Sam68 fusion constructs, except for GFP-Sam68:I→N-nuclear localization signal (NLS) and GFP-Sam68ΔC, were generated by subcloning the *Eco*RI fragments of corresponding myc-Sam68 constructs into pEGFP-C1 (Clontech, Palo Alto, CA). myc-Sam68f, Sam68Δ1-67 (initially called p62), Sam68ΔN, Sam68ΔKH, Sam68ΔL1, Sam68ΔL4, Sam68:G→D (GLD-1 missense mutation), Sam68:I→N (human FMR1 missense mutation), Sam68:E→G (mouse Qk1 missense mutation), and Sam68:2G→R (GLD-1 missense mutation) have been described previously (Richard *et al.*, 1995; Chen *et al.*, 1997). myc-Sam68ΔKH isoform (Sam68 splice variant), Sam68:NF→DL, Sam68:R→C (Who/How missense mutation), Sam68:R→A (putative Sam68 NLS disruption), Sam68:D→N (GLD-1 missense mutation), Sam68:A→T (GLD-1 missense mutation), Sam68:P→L (GLD-1 missense mutation), and Sam68ΔL1-NF were generated by inverse PCR using myc-Sam68f as the DNA template and the following oligonucleotide pairs as primers: 5′-GAG GAA GAG TTG CGC AAG GGT-3′ and 5′-CTT TGG ATA CTG CTT GAC AGG-3′ (for myc-Sam68ΔKH isoform); 5′-GAC CTT GTG GGG AAG ATT CTT GGA-3′ and 5′-GAA CTT TGG ATA CTG CTT GAC-3′ (for myc-Sam68:NF→DL); 5′-TGC GAC AAA GCC AAG GAG GAA-3′ and 5′-CAT TGA ACC CTT CCC CAA GAC-3′ (for myc-Sam68:R→C); 5′-TCC GCA CCA GTG AAG GGA GCA TAC-3′ and 5′-TCC AGG AGC CTT CAG TGA TGG CCT-3′ (for myc-Sam68:R→A); 5′-AAG CAG TAT CTA AAG TTC AAT TTT-3′ and 5′-GAC AGG TAT CAG CAC GCG TTC-3′ (for myc-Sam68:P→L); 5′-ACT ATG GAA GAA GTC AAG-3′ and 5′-ACG GGC CAT AAG AGC ATA-3′ (for myc-Sam68:A→T); 5′-AAT ATC TGT CAG GAG CAG-3′ and 5′-ATC CAT CAT ATC TGG TAC-3′ (for myc-Sam68:D→N); and 5′-AAT TTT GTG GGG AAG ATT-3′ and 5′-GAC AGG TAT CAG CAC GCG TTC-3′ (for myc-Sam68ΔL1NF). (Underlined nucleotides denote changes introduced.)

GFP-Sam68:I→N-NLS was constructed by a two-step subcloning strategy. The NLS sequence was first introduced into a DNA frag-

ment encoding the C-terminal 113 amino acids of Sam68 by PCR amplification with myc-Sam68f as the DNA template and the following oligonucleotides as primers: 5′-CTT GAA TTC AGT ACC TGA ACC CTC TCG-3′ and 5′-TCA GAA TTC *ACA CCT TAC GCT TCT TCT TTG* GAT GCT CTC TGT ATG CTC CCT TCA CTG G-3′. (The *Eco*RI site is underlined and the sequence encoding the SV40 large T antigen NLS, PKKKRKV [Kalderon *et al.*, 1984], is italicized.) The amplified DNA fragment was digested with *Eco*RI and *Xho*I (an internal *Xho*I site was used) and subcloned into the corresponding sites of pEGFP-C1, generating GFP-NLS. The *Xho*I fragment of GFP-Sam68:I→N was then inserted into the *Xho*I site of GFP-NLS, generating GFP-Sam68:I→N-NLS. GFP-Sam68ΔC was constructed by subcloning the *Sac*I fragment of myc-Sam68f into the corresponding *Sac*I site in pEGFP-C1. GFP-SLM-1 and GFP-SLM-2 were described previously (Di Fruscio *et al.*, 1999). The construct encoding GFP-polypyrimidine tract–binding protein (PTB) was generated by subcloning the PTB cDNA (Patton *et al.*, 1991; kindly provided by Nahum Sonenberg, McGill University) into the *Bgl*II and *Sma*I sites of pEGFP-C1. All GFP fusion constructs produce proteins with GFP fused to their N termini. The identities of the plasmid constructs were verified by dideoxynucleotide sequencing with Sequenase (United States Biochemical, Cleveland, OH).

Antibodies

The Sam68 mAb 7-1 (sc-1238), the Sam68 rabbit polyclonal antibody C-20 (sc-333), the PML mAb PG-M3 (sc-966), and the SMRT goat polyclonal antibody N-20 (sc-1610) were purchased from Santa Cruz Biotech (Santa Cruz, CA). The anti-tubulin mAb B-5-1-2 was from Sigma Chemical (St. Louis, MO). The anti-SMN mAb was purchased from Transduction Laboratories (Lexington, KY). Anti-bromodeoxyuridine (BrdU) mAb (BMC9318) was purchased from Boehringer Mannheim (Indianapolis, IN). Anti-SC35 mAb was purchased from PharMingen (San Diego, CA). Anti-coilin rabbit polyclonal antibody was kindly provided by Edward Chan (Andrade *et al.*, 1993), the anti-fibrillarin mAb 72B9 was kindly provided by Michael Pollard (Scripps Institute, La Jolla, CA), and the Y12 mouse mAb was kindly provided by Mark Bedford (Harvard University, Cambridge, MA). We generated a new rabbit anti-Sam68 antibody (AD1). Rabbits were immunized with a peptide encompassing amino acids 330–348 of Sam68 (RGVPPPPTVRGAPTPRAR) covalently coupled to keyhole limpet hemocyanin. The 9E10 anti-myc mAb was from the American Type Culture Collection (Rockville, MD). Goat anti-mouse and goat anti-rabbit rhodamine-conjugated antibodies were purchased from Pierce (Rockford, IL). Goat anti-mouse and goat anti-rabbit FITC-conjugated antibodies were from Jackson Laboratories (Bar Harbor, ME).

Cell Culture and Transient Transfection

HeLa cells were maintained in DMEM (Life Technologies-BRL, Grand Island, NY) supplemented with 2 mM L-glutamine, 1 mM sodium pyruvate, 100 U/ml penicillin, 100 μg/ml streptomycin (all from ICN, Costa Mesa, CA), and 10% bovine calf serum (Hyclone, Logan, UT). Cells were maintained at 37°C in 5% CO_2. The day before transfection, the cells were plated on glass coverslips at a density of 10^5 cells per 22-mm^2 coverslip (Fisher Scientific, Nepean, Ontario, Canada). DNA transfections of GFP plasmids were performed with the use of the LipofectAMINE PLUS reagent (Life Technologies-BRL) according to the manufacturer's instructions. The transfection of myc-Sam68 into HeLa cells was carried out with the T7 vaccinia virus system as previously described (Richard *et al.*, 1995). The other cell lines used in this study were maintained as suggested by the American Type Culture Collection.

Labeling of Transcription Sites in Permeabilized Cells

Labeling of RNA synthesis sites was done according to published methods (Jackson *et al.*, 1993; Pombo *et al.*, 1998) with modifications. Briefly, HeLa cells grown on coverslips were transfected with GFP-Sam68, GFP-Sam68ΔL1, or GFP-PTB. Twelve hours after transfection, the cells were washed once with 1× PBS, once with a "physiological" buffer (100 mM potassium acetate, 30 mM KCl, 10 mM Na_2HPO_4, 1 mM $MgCl_2$, 1 mM ATP, 1 mM DTT, 0.2 mM PMSF, 10 U/ml RNAguard RNase inhibitor, and 100 μg/ml BSA), and then permeabilized with 50 μg/ml saponin in physiological buffer for 5 min at 4°C. The permeabilized cells were rinsed with ice-cold physiological buffer and immediately incubated with physiological buffer supplemented with 0.1 mM ATP, CTP, GTP, and Br-UTP for 20 min at 33°C. After rinsing with ice-cold physiological buffer, the cells were fixed with 4% paraformaldehyde, permeabilized with 1% Triton X-100, and immunostained with anti-BrdU mAb, which also cross-reacts with Br-UTP, followed by a rhodamine-conjugated goat anti-mouse secondary antibody.

Immunofluorescence and Confocal Microscopy

Transfected or untransfected cells were fixed with 4% paraformaldehyde in 1× PBS for 5 min at room temperature and permeabilized with either 1% Triton X-100 in PBS for 5 min at room temperature or 50% methanol:50% acetone for 15 min at −20°C. If the cells were to be visualized only for GFP, then the glass cover slide was mounted onto glass slides with glycerol containing 3 μg/ml DAPI to stain the nuclei. If the cells required antibody staining, the permeabilized cells were blocked with 10% calf serum (Hyclone) in PBS for 30 min at room temperature, the primary antibodies were incubated at room temperature for 1 h in PBS containing 3% BSA, anti-SMN (1:20), anti-PML (1:50), anti-coilin (1:500), anti-tubulin (1:200), anti-myc ascites (1:500), anti-fibrillarin tissue culture supernatant (1:20), anti-Y12 tissue culture supernatant (1:1), anti-SC35 (1:100), anti-BrdU (6 μg/ml), anti-Sam68 C-20 and AD1 (1:200), and anti-Sam68 7-1 (1:20). The cells were washed extensively with PBS and incubated with the appropriate secondary antibodies (1:200) in PBS containing 3% BSA for 20 min. The cells were washed and mounted onto glass slides as described above. The cells were visualized with a Leitz (Wetzlar, Germany) Aristoplan fluorescence microscope or by confocal microscopy.

Correlative Microscopy and Electron Microscopy

Detailed descriptions of the electron microscopy procedure are presented elsewhere (Bazett-Jones and Hendzel, 1999). Briefly, HeLa cells were grown on plastic caps, fixed with 1% paraformaldehyde in PBS, permeabilized with 0.5% Triton X-100 in PBS, and labeled with immunofluorescence using anti-Sam68 AD1 rabbit polyclonal antibodies. The cells were then refixed in 2% glutaraldehyde in PBS for 5 min and dehydrated in ethanol, starting at 30%, before embedding in Quetol 651 resin. Sections of ~30 nm thickness were obtained by ultramicrotomy with a diamond knife (Drukker, Cuijk, The Netherlands). The sections were placed directly onto finder grids. Electron micrographs were obtained with a Gatan (Pleasanton, CA) 14-bit slow-scan cooled charge-coupled device detector on a Carl Zeiss (Thornwood, NY) EM 902 transmission electron microscope equipped with an imaging spectrometer.

RESULTS

Sam68, SLM-1, and SLM-2 Localize in Nuclear Dots

Sam68 has been shown to be present in membranes and the nucleus of NIH 3T3 cells (Wong *et al.*, 1992; Ishidate *et al.*, 1997). To further examine the subcellular localization of Sam68, we carried out indirect immunofluorescence studies in HeLa cells with three different anti-Sam68 antibodies. The Sam68 antibodies were mouse mAb 7-1 as well as rabbit polyclonal antibodies C-20 (Taylor and Shalloway, 1994) and AD1. mAb 7-1 is Sam68 specific, whereas C-20 recognizes

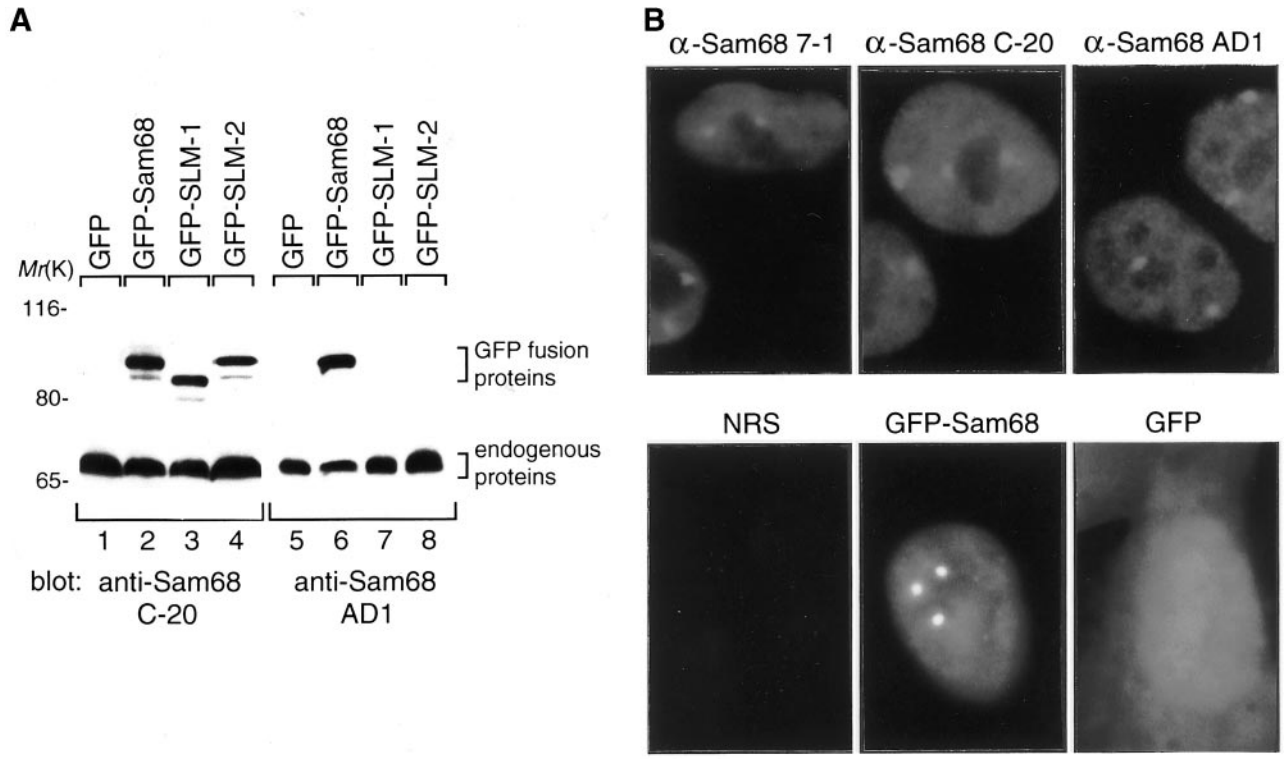

Figure 1. Sam68 localizes in nuclear bodies. (A) Anti-Sam68 AD1 recognizes Sam68 but not SLM-1 and SLM-2. HeLa cells transfected with GFP alone, GFP-Sam68, GFP-SLM-1, or GFP-SLM-2 were lysed and the cell lysates were divided equally, resolved by SDS-PAGE, transferred to nitrocellulose membranes, and immunoblotted with anti-Sam68 C-20 (lanes 1–4) or AD1 (lanes 5–8) antibodies. The migration of endogenous and GFP-Sam68/SLM proteins is indicated on the right, and the positions of molecular mass markers (in kilodaltons) are shown on the left. (B) HeLa cells were fixed, permeabilized, and immunostained with anti-Sam68 mAb 7-1, rabbit polyclonal Sam68/SLM C-20 antibody, rabbit polyclonal antibody AD1, or normal rabbit serum (NRS), followed by a rhodamine-conjugated goat anti-mouse or anti-rabbit secondary antibody, and visualized by fluorescence microscopy. Expression vectors encoding GFP-Sam68 or GFP alone were transfected into HeLa cells, and 12 h after transfection, live cells were visualized by fluorescence microscopy.

Sam68, SLM-1, and SLM-2 (Di Fruscio *et al.*, 1999). AD1 is a Sam68-specific antibody that we generated against a peptide containing amino acids 330–348 of mouse Sam68. The specificity of this antibody is depicted in Figure 1A. HeLa cells expressing GFP fusion proteins of Sam68, SLM-1, and SLM-2 were lysed, divided equally, and analyzed by immunoblotting with either rabbit C-20 or AD1 antibody. C-20 recognized GFP-Sam68, GFP-SLM-1, and GFP-SLM2, whereas AD1 recognized only GFP-Sam68. A band at 68 kDa was observed in both C-20 and AD1 immunoblots that corresponds to endogenous Sam68/SLM proteins. The band at 68 kDa in the AD1 immunoblots was less intense than the corresponding band in the C-20 lanes, consistent with our immunodepletion studies demonstrating that C-20 recognizes other proteins at 68 kDa that may be SLM-1, SLM-2, or yet unidentified SLMs (Di Fruscio *et al.*, 1999).

To examine the localization of endogenous Sam68, the antibodies were used in indirect immunofluorescence studies in HeLa cells. All three anti-Sam68 antibodies gave a similar pattern, a diffuse nucleoplasmic staining with approximately two to five prominent nuclear dots, that was not observed with normal rabbit serum (Figure 1B). C-20 antibody gave a stronger diffuse nucleoplasmic signal, which most likely reflected the immunostaining of both Sam68 and SLM proteins. The strong nucleoplasmic staining made the nuclear dots less prominent, which may be one of the reasons that the nuclear dots were not detected in previous studies (see DISCUSSION). Plasmids expressing GFP alone or GFP-Sam68 were transfected in HeLa cells, and the cells were visualized live using fluorescence microscopy. GFP-Sam68 displayed an expression pattern identical to that observed with endogenous Sam68, whereas GFP alone was expressed diffusely throughout the cell (Figure 1B). Taken together, these findings demonstrate that the localization of Sam68 into nuclear dots was not an artifact of overexpression, fixation, and/or immunostaining procedures.

We next investigated whether the closely related Sam68 family members SLM-1 and SLM-2 also concentrated in nuclear dots. HeLa cells transfected with GFP-SLM-1 and GFP-SLM-2 were immunostained with anti-Sam68 AD1 antibody, and colocalization was determined by confocal microscopy. GFP-SLM-1 displayed a localization pattern similar to that of Sam68: diffuse extranucleolar staining with one to five distinct nuclear dots (Figure 2a), and these dots colocalized with endogenous Sam68 nuclear dots (Figure 2c, arrows). GFP-SLM-2 displayed three major localization patterns: ~40% of transfected cells exhibited a pattern similar to that of Sam68 and SLM-1 (Figure 2d), another ~40% of

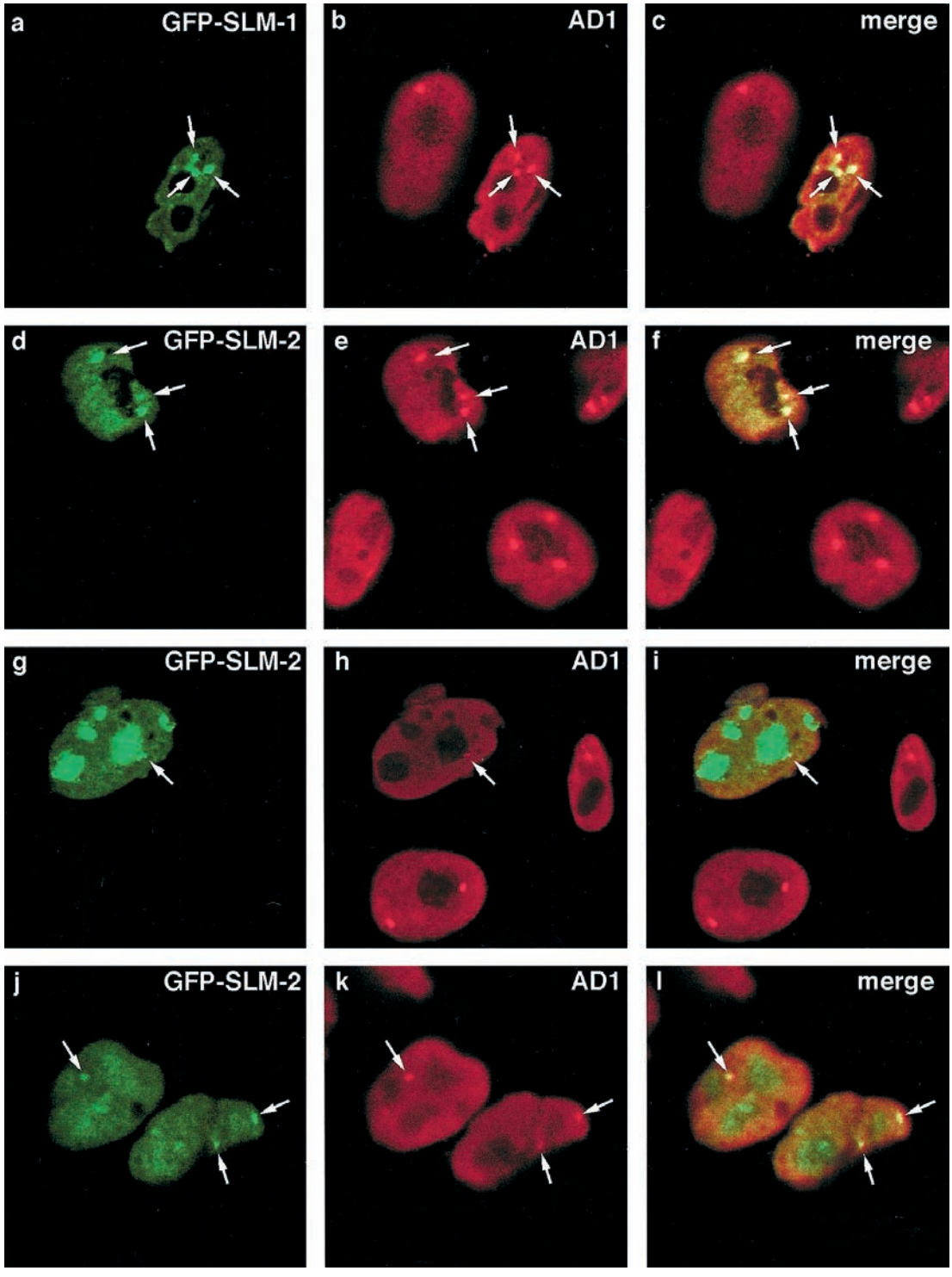

Figure 2. GFP-SLM-1 and GFP-SLM-2 colocalize with Sam68 in nuclear bodies. GFP-SLM-1 (a–c) and GFP-SLM-2 (d–l) were transfected individually in HeLa cells, and the cells were fixed, permeabilized, and immunostained with anti-Sam68 AD1 antibody followed by a rhodamine-conjugated goat anti-rabbit secondary antibody (b, e, h, and k). Colocalization was determined by confocal microscopy, and the merged images are shown on the right (c, f, i, and l). The arrows point to nuclear bodies that colocalize. Three major localization patterns were observed with GFP-SLM-2: extranucleolar staining (d), accumulation in nucleoli (g), and diffuse staining in both nucleoplasm and nucleoli (j).

Table 1. Prevalence of Sam68 nuclear dots in different cell lines

Cell line	Description	SNB prevalence[a] (%)
HeLa	Human cervical carcinoma epithelial cell	88.7
BT-20	Human breast carcinoma epithelial cell	89.1
Hs 578T	Human breast carcinoma epithelial cell	48.6
MCF-7	Human breast adenocarcinoma epithelial cell	4.8
SK-N-MC	Human neuroblastoma cell	0.7
293	Human embryo kidney cell transformed with adenovirus 5	4.5
HF-7650	Human fibroblast cell	0
AtT-20	Mouse pituitary tumor cell	1.3
Neuro-2A	Mouse neuroblastoma cell	0.4
NIH 3T3	Mouse embryo fibroblast cell	5.6
Src 3T3	NIH 3T3 cell transformed with v-Src	7.2
MEF	Primary mouse embryo fibroblast cell	0.9
C6 glioma	Rat glioma cell	1.1
GH3	Rat pituitary tumor cell	0.8
Rat1	Rat connective tissue epithelial cell	0.5
REF-52	Rat embryo fibroblast cell	0.5

[a] Different cell lines grown on coverslips were fixed, permeabilized, and immunostained with anti-Sam68 AD1 antibody followed by a rhodamine-conjugated secondary antibody. For each cell line, an average of 250–300 cells from two independent experiments were counted, and SNB prevalence is defined as the percentage of cells that contain one or more SNBs.

transfected cells had GFP-SLM-2 accumulated in the nucleoli with relatively weak nucleoplasmic staining (Figure 2g), and the remaining ~20% of transfected cells showed evenly diffuse staining throughout the nucleus, including both the nucleoplasm and the nucleoli (Figure 2j). Nuclear dots were observed in all three localization patterns of GFP-SLM-2, and they always colocalized with Sam68 nuclear dots (Figure 2, f, i, and l, arrows). These data suggest that Sam68 nuclear dots also contain SLM-1 and SLM-2.

A panel of human, mouse, and rat cell lines was examined for the presence of Sam68 nuclear dots using indirect immunofluorescence with anti-Sam68 antibodies. Sam68 nuclear dots were predominantly present in some, but not all, human transformed cell lines. Approximately 50–90% of HeLa (human cervical cancer), BT-20 (human breast cancer), and Hs578T (human breast cancer) cells contained Sam68 nuclear dots (Table 1). Sam68 nuclear dots were rarely found (~1–7%) in immortalized cells such as NIH 3T3 or other transformed cell lines examined, such as v-Src–transformed 3T3 cells, SK-N-MC, MCF-7, C6 glioma, GH3, Neuro-2A, AtT-20, and 293. Normal fibroblasts, including HF-7650, MEF, Rat1, and REF-52 cells, did not have Sam68 nuclear dots (<1%). Overexpression of GFP-Sam68 in NIH 3T3 and REF-52 cells did not induce the formation of nuclear dots (our unpublished results), suggesting that the presence or absence of Sam68 nuclear dots is not due to different levels of Sam68 expression in different cell lines. These findings imply that immortalization and/or transformation is a prerequisite for the appearance of Sam68 nuclear dots but that Sam68 nuclear dots are not a general marker for transformation or cancer.

Sam68 Nuclear Bodies Are Novel Nuclear Structures

The Sam68 nuclear dots resembled nuclear bodies in number and size. Confocal microscopy studies were initiated to investigate whether Sam68 nuclear dots were coiled bodies, gems, or PML nuclear bodies. HeLa cells were double immunostained with anti-Sam68 antibodies and anti-coilin, anti-SMN, or anti-PML antibodies. Colocalization of rhodamine-stained (red) Sam68 nuclear dots and fluorescein-stained (green) coiled bodies, gems, or PML nuclear bodies was analyzed by confocal microscopy. Sam68 nuclear dots did not colocalize with coiled bodies, gems, or PML nuclear bodies (Figure 3). Occasionally, Sam68 nuclear dots were adjacent to or even partially overlapped coiled bodies or gems. The large arrow in Figure 3f indicates partial overlapping with a gem. The significance of this overlap is unknown; the overlap may be a chance occurrence, given that overlapping was infrequently observed. Taken together, these studies suggest that Sam68 nuclear dots are novel nuclear structures distinct from coiled bodies, gems, and PML nuclear bodies. The Sam68 nuclear dots were also distinct from the perinucleolar compartment (PNC), as visualized with GFP-PTB (Huang *et al.*, 1997) and anti-Sam68 antibodies (our unpublished results). Sam68 nuclear dots as well as nucleoplasmic Sam68 did not colocalize with fibrillarin (our unpublished results), a marker for coiled bodies and the nucleolus (Lamond and Earnshaw, 1998). Based on the uniqueness of Sam68 nuclear dots, we named them Sam68/SLM nuclear bodies (SNBs).

SNBs Are Dynamic Structures

The dynamic nature of SNBs and their cell cycle regulation were investigated. Unsynchronized HeLa cells were immunostained with anti-Sam68 antibodies, and cells in interphase and various stages of mitosis, identified by chromatin morphology with DAPI staining, were examined for the presence of SNBs (Figure 4A). In interphase cells, Sam68 exhibited a diffuse extranucleolar pattern with several SNBs in each nucleus (Figure 4Aa, lower cell). In early prophase, Sam68 remained confined to the nucleus and SNBs were visible (Figure 4A, a and f). SNBs disassembled in mid to late prophase (Figure 4A, b and g) before the breakdown of the nuclear membrane. In metaphase (Figure 4A, c and h) and anaphase (Figure 4A, d and i), Sam68 was diffusely localized throughout the cell and no SNBs were visible. Of note, Sam68 did not colocalize with the chromosomes. During late telophase and/or early G1 phase, SNBs reappeared in the daughter cells (Figure 4A, e and j). These findings demonstrate that SNBs are dynamic structures that disassemble during mitosis.

Transcriptional inhibition has been shown to influence the integrity of several nuclear structures, including coiled bodies and gems (Carmo-Fonseca *et al.*, 1993; Liu and Dreyfuss, 1996). The effect of transcriptional inhibition on SNBs was examined. After 3 h of treatment with 5 μg/ml actinomycin D, a concentration known to inhibit RNA polymerases I and II, Sam68 immunostaining became less diffuse in the nucleoplasm and SNBs disassembled (Figure 4Bb). SNBs also

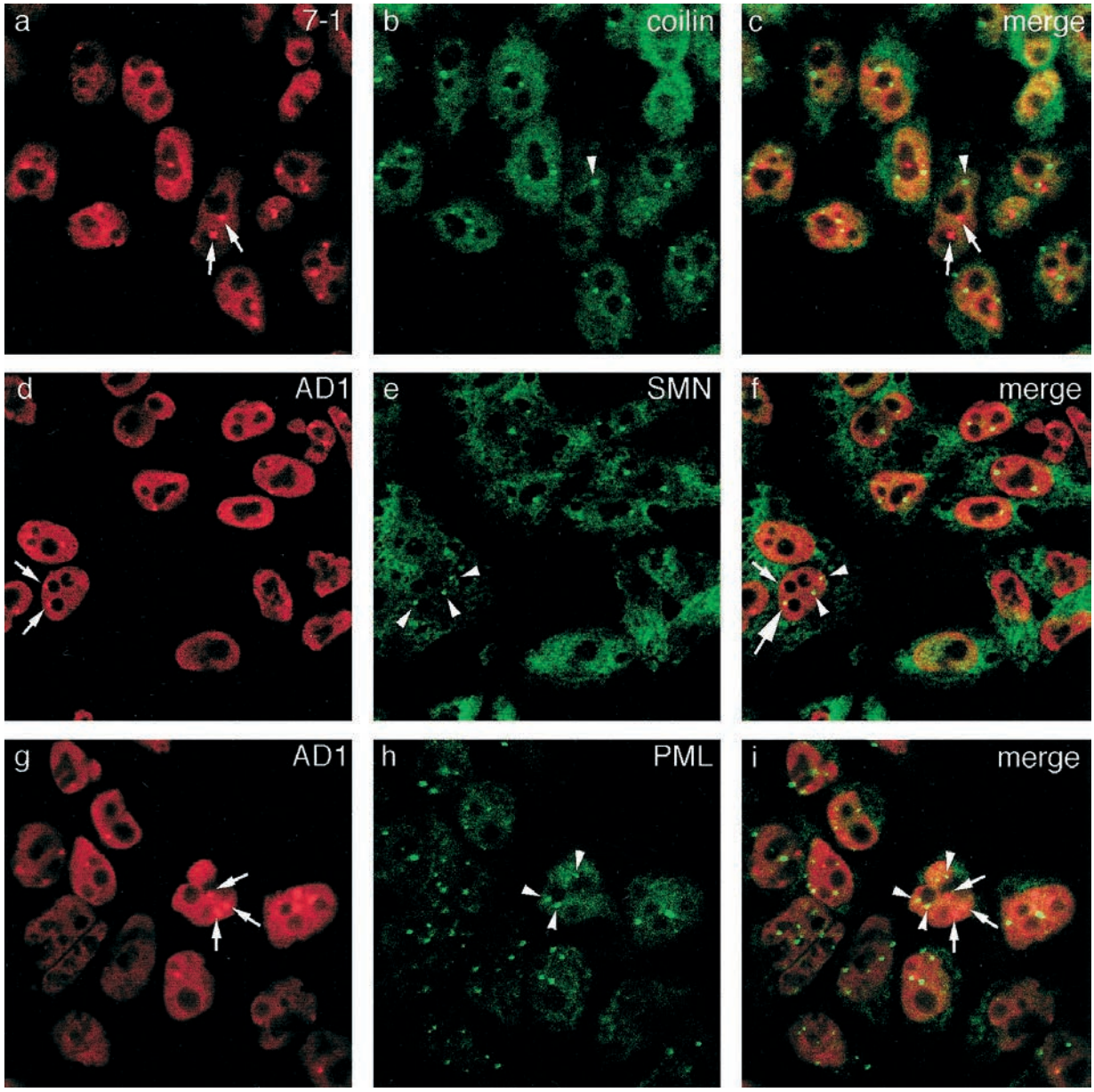

Figure 3. Sam68 nuclear bodies are novel nuclear structures. HeLa cells were fixed, permeabilized, and double immunostained with anti-Sam68 7-1 and anti-coilin (a–c), anti-Sam68 AD1 and anti-SMN (d–f), or anti-Sam68 AD1 and anti-PML (g–i). Anti-Sam68 antibodies were followed by rhodamine-conjugated secondary antibodies (left panels), and the other antibodies were followed by FITC-conjugated secondary antibodies (middle panels). Colocalization was determined by merging the confocal images of the left and middle panels using confocal microscopy (right panels). Sam68 nuclear bodies are indicated by arrows, and coiled bodies, gems, and PML nuclear bodies are indicated by arrowheads. The large arrow in panel f indicates partial overlap between a Sam68 nuclear body and a gem.

disassembled when HeLa cells were treated with 50 μg/ml α-amanitin, another transcription inhibitor, for 5 h (our unpublished results). The treatment of HeLa cells with the protein synthesis inhibitor cycloheximide had no effect on the structural integrity of SNBs (Figure 4Bc). These observations suggested that the integrity of SNBs was dependent on transcription but not on ongoing protein synthesis. Because cycloheximide also inhibits the transcriptional activity of RNA polymerase I (Willems *et al.*, 1969), the fact that SNBs were resistant to cycloheximide treatment suggested that the structure of SNBs was most likely dependent on the activity of RNA polymerase II but not RNA polymerase I. To exclude the interference of the fixation procedures, we examined GFP-Sam68 in living cells. Actinomycin D treatment caused the GFP-Sam68 nuclear bodies to disassemble (our unpublished results).

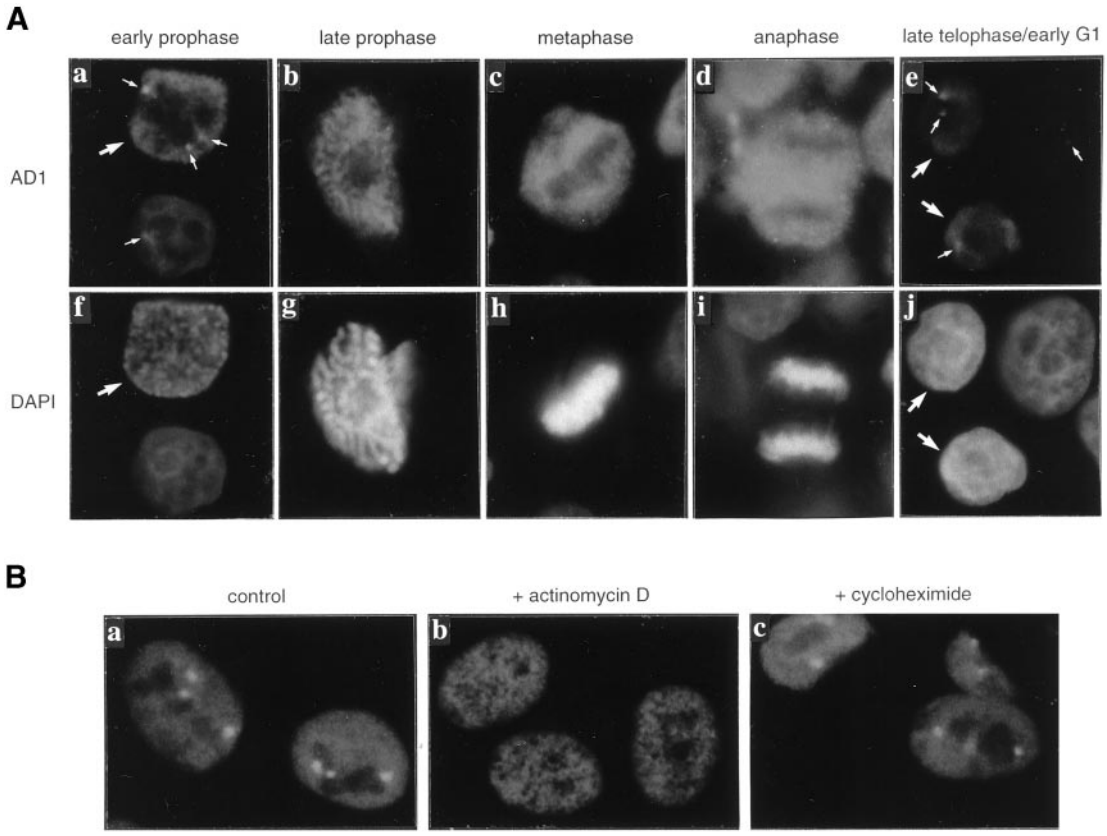

Figure 4. Sam68 nuclear bodies are dynamic structures. (A) HeLa cells were fixed, permeabilized, and immunostained with anti-Sam68 AD1 antibody followed by rhodamine-conjugated goat anti-rabbit secondary antibody, and the cell nuclei were stained with DAPI. Fluorescence of representative cells in interphase (a and f, lower cells; e and j, right cells), early prophase (a and f, large arrow), late prophase (b and g), metaphase (c and h), anaphase (d and i), and late telophase/early G1 phase (e and j, large arrows) are shown. Sam68 nuclear bodies are indicated by small arrows. (B) HeLa cells were mock-treated or treated with 5 μg/ml actinomycin D (b) or 20 μg/ml cycloheximide (c) for 3 h, then fixed, permeabilized, and immunostained with anti-Sam68 AD1 antibody.

Taken together, these results further indicated that SNBs, like nuclear bodies, are dynamic structures whose organization changes with metabolic states.

GSG Domain Mutations and Deletions Alter Sam68 Localization

Because many genetic mutations have been identified in the GSG and KH domains, we investigated the role of the Sam68 GSG/KH domain in protein localization. GFP-Sam68 fusion proteins containing missense mutations or deletions within the GSG domain were examined for altered cellular localization. Interestingly, different Sam68 localization patterns were observed (Figure 5A), and the Sam68 mutants were grouped into six different classes based on their localization patterns (Figure 5B).

In class I, all transfected cells displayed the wild-type Sam68 expression pattern, a diffuse nucleoplasmic staining with several SNBs (pattern A). Sam68 alanine 247 in the KH domain and aspartic acid 262 at the C-terminal-to-KH-domain region (CK region; Figure 5B) are conserved amino acids in the GSG domain, and missense mutations for these amino acids have been isolated in GLD-1 (Jones and Schedl, 1995). Mutation of Sam68:A247T and Sam68:D262N displayed wild-type cellular Sam68 distribution, suggesting that these amino acid changes had no effect on Sam68 protein localization.

In class II, ~90% of the Sam68:P168L-transfected cells displayed a wild-type Sam68 localization pattern (pattern A) and ~10% of cells concentrated Sam68:P168L in 10–30 SNBs (pattern B). Sam68 proline 168, located in loop 1 of the Sam68 KH domain, is fully conserved in the GSG domain, and this point mutation isolated in GLD-1 reverses the gain-of-function sex determination phenotype of the glycine 248-to-arginine mutation and displays the loss-of-function defective oogenesis (Jones and Schedl, 1995). The GFP-Sam68:P168L protein implicates the KH domain loop 1 in Sam68 cellular localization.

In class III, ~90% of the cells transfected with Sam68ΔL1, Sam68:NF→DL, Sam68ΔL1NF, or Sam68:R204C displayed exclusive SNBs (pattern B) and ~10% of the cells showed a wild-type Sam68 pattern (pattern A). In addition to the six-amino acid deletion in KH domain loop 1, asparagine 171 and phenylalanine 172 were substituted to aspartic acid and leucine, respectively, in Sam68ΔL1. Therefore, to deter-

mine whether it was the deletion or the substitutions that altered Sam68 localization, we constructed a protein containing only the deletion (Sam68ΔL1NF) and another harboring the two amino acid substitutions (Sam68:NF→DL). Either the substitution of fully conserved amino acids 171 and 172 (Sam68:NF→DL) or the deletion of loop 1 (Sam68ΔL1NF) was sufficient to concentrate the proteins exclusively in SNBs. These data demonstrate that Sam68 KH domain loop 1 is involved in protein localization. We have shown that Sam68ΔL1 has impaired self-association capabilities, with no effect on RNA binding (Chen *et al.*, 1997). Because the RNA-binding properties of Sam68ΔL1 are normal, this suggests that the protein localization property of the Sam68 GSG domain is separate from its RNA-binding activity. The substitution of R204C in Sam68 KH domain loop 4 also resulted in ~90% of the cells containing only SNBs. This missense mutation identified in Who/How has been shown to result in flies with the wings-held-out phenotype (Baehrecke, 1997). Interestingly, this missense mutation, when introduced in Who/How, did not alter RNA binding and self-association (Chen and Richard, 1998), suggesting that the molecular defect of this missense mutation may be in protein localization.

In class IV, cells transfected with Sam68ΔKH, Sam68ΔKH isoform, Sam68ΔL4, or Sam68:2G→R displayed three major expression patterns: ~30% of the cells displayed only SNBs (pattern B), ~50% of cells showed punctate staining throughout the entire cell (pattern C), and the remaining ~20% had distinct cytoplasmic punctate staining (pattern D). The cytoplasmic punctate staining observed may represent Sam68 localization to specific organelles. Using double staining with Lysotracker Red, we have observed that the Sam68 punctate staining does not represent lysosomes (our unpublished results). Sam68ΔKH contains a 60-amino acid deletion that removes a large portion of the KH domain. This deletion completely altered the localization of Sam68, as none of the cells expressing Sam68ΔKH displayed the wild-type Sam68 expression pattern. A rare natural isoform of Sam68, Sam68ΔKH isoform, has been discovered and contains a 39-amino acid deletion in the Sam68 KH domain (Barlat *et al.*, 1997). A GFP fusion protein containing this isoform had similar expression patterns as those observed with GFP-Sam68ΔKH. The deletion of KH domain extended loop 4 (Sam68ΔL4) or the replacement of glycines 199 and 201 in loop 4 with arginines (Sam68:2G→R) also exhibited expression patterns identical to those observed with Sam68ΔKH. These data further implicate the KH domain in protein localization, with a specific requirement for loop 4. Our findings are consistent with previous results showing that deletion of the Sam68 KH domain results in accumulation in nuclear dots (McBride *et al.*, 1998).

In class V, the cellular localization of two RNA-binding defective Sam68 proteins was examined. One mutation altering the equivalent substitution of GLD-1 glycine 227 to aspartic acid (Jones and Schedl, 1995) and the second altering the equivalent substitution of FMR1 isoleucine 304 to asparagine (DeBoulle *et al.*, 1993) were introduced in Sam68. GFP-Sam68:G→D and GFP-Sam68:I→N displayed expression patterns similar to those observed with GFP-Sam68ΔKH, except a larger percentage of cells showed a cytoplasmic distribution (pattern D) and a smaller percentage of cells showed an entire cell distribution (pattern C). In addition, a considerable number of cells (~25% for Sam68:G→D and ~7% for Sam68:I→N) displayed a cytoplasmic fibrous pattern characteristic of microtubules that was unique to these two Sam68 proteins (pattern E). The GLD-1 glycine 227-to-aspartic acid point mutation has been shown to result in germline tumors (Jones and Schedl, 1995). The human FMR1 isoleucine 304-to-asparagine mutation results in severe mental retardation (DeBoulle *et al.*, 1993). FMR1:I304N has been shown to alter the structure of the KH domain (Musco *et al.*, 1996), impair the ability of FMR1 to associate with RNA (Siomi *et al.*, 1994), and prevent FMR1 from associating with polyribosomes (Feng *et al.*, 1997). We have previously shown that the introduction of these point mutations in Sam68 alters its ability to bind homopolymeric and cellular RNA (Chen *et al.*, 1997). Because both Sam68:G→D and Sam68:I→N self-associated (Chen *et al.*, 1997), we reasoned that the altered protein localization patterns observed were independent of self-association.

In class VI, the lethal point mutation identified in the Qk1 GSG domain was introduced in the N-terminal-to-KH-domain (NK) region of Sam68 (Sam68:E→G). GFP-Sam68:E→G also exhibited several patterns of expression. A large fraction of cells (~47%) showed punctate cytoplasmic staining (pattern D) and a small fraction (~6%) showed punctate staining throughout the entire cell (pattern C). Additionally, many cells (~24%) displayed a wild-type Sam68 expression pattern (pattern A) and an equal number of cells (~22%) displayed diffuse staining in both the nucleus and the cytoplasm (pattern G). Because the Sam68:E→G protein has wild-type RNA binding and self-association properties (Chen *et al.*, 1997), the localization property of the Sam68 GSG domain is separate from its ability to bind RNA and self-associate.

The Sam68 C Terminus and the GSG Domain Are Both Required for Nuclear Localization

The primary amino acid sequence of Sam68 does not reveal any known NLS or nuclear export sequence. A putative NLS has been identified at the C terminus of Sam68, and the substitution of Sam68 arginine 429 with alanine in the putative NLS has been shown to result in a diffuse distribution throughout the entire cell (Ishidate *et al.*, 1997). To examine the role of this putative NLS in Sam68 protein localization, the C terminus of Sam68 was truncated to remove the tyrosine-rich region and the putative NLS (Sam68ΔC). The plasmid encoding this protein was transfected in HeLa cells, and GFP-Sam68ΔC was visualized by fluorescence microscopy. Transfected cells expressing GFP-Sam68ΔC displayed diffuse cytoplasmic staining (Figure 5A, pattern F). Similar results were obtained when only the last 4 or 11 amino acids were deleted at the C terminus of Sam68 (our unpublished results). Moreover, the substitution of Sam68 arginine 429 with alanine (Sam68:R→A) resulted in a distribution pattern similar to that of GFP alone (Figure 5A, pattern G), consistent with previous studies (Ishidate *et al.*, 1997). In contrast, deletion of 67 or 102 amino acids at the N terminus of Sam68 (Sam68Δ1-67 and Sam68ΔN) showed no effect on Sam68 localization (Figure 5B). These results demonstrate that the C-terminal region of Sam68, but not the N-terminal region, plays a role in Sam68 protein localization. To determine whether the GSG domain played a dominant role in protein localization, a sequence encoding the SV40 large T antigen

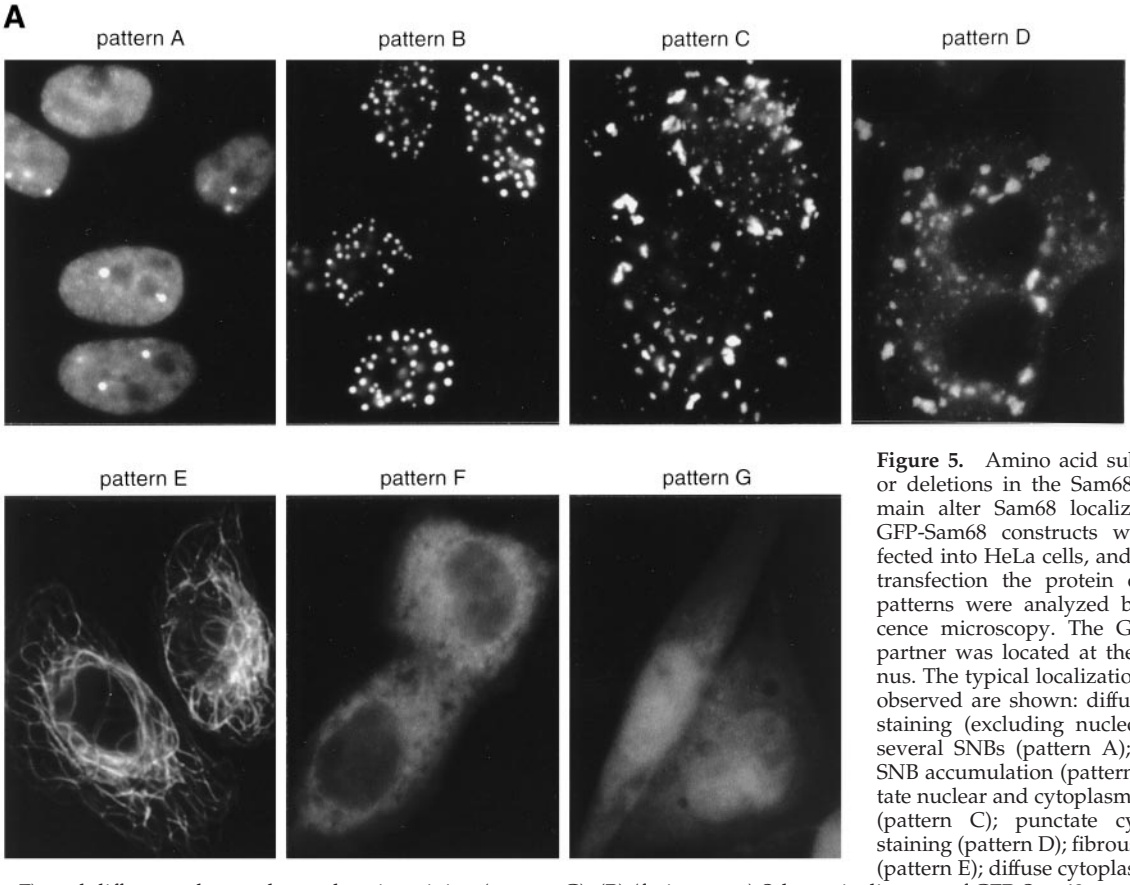

Figure 5. Amino acid substitutions or deletions in the Sam68 GSG domain alter Sam68 localization. (A) GFP-Sam68 constructs were transfected into HeLa cells, and 12 h after transfection the protein expression patterns were analyzed by fluorescence microscopy. The GFP fusion partner was located at the N terminus. The typical localization patterns observed are shown: diffuse nuclear staining (excluding nucleolus) with several SNBs (pattern A); exclusive SNB accumulation (pattern B); punctate nuclear and cytoplasmic staining (pattern C); punctate cytoplasmic staining (pattern D); fibrous structure (pattern E); diffuse cytoplasmic staining (pattern F); and diffuse nuclear and cytoplasmic staining (pattern G). (B) (facing page) Schematic diagram of GFP-Sam68 constructs and the quantitation of different localization patterns. In the diagrams of the constructs, the GSG domain is depicted with a bracket. The GSG domain contains an extended KH domain (denoted by the black box). The regions in the GSG domain at the N terminus of the KH domain and at the C terminus of the KH domain were called the NK and CK regions, respectively. The genes in which the genetic missense mutations were identified that alter amino acids in the GSG or KH domain are shown on the left. Δ indicates a deletion; → represents an amino acid substitution; and a horizontal or vertical thin line denotes the position of a deletion or point mutation. The NLS represents the SV40 large T antigen nuclear localization sequence (PKKKRKV). For each construct, an average of 250–300 transfected (green) cells from three separate experiments were counted, and the localization patterns were expressed as percentages. The Sam68 proteins harboring amino acid substitutions or deletions in their GSG mutations were grouped into six phenotypic classes based on their localization patterns.

NLS was introduced at the C terminus of Sam68:I→N (Sam68: I→N-NLS). Interestingly, this protein was not localized to the nucleus but displayed the typical pattern observed with Sam68:I→N (Figure 5B). As a control, the introduction of the SV40 large T antigen NLS at the C terminus of GFP targeted the fusion protein to the nucleus (our unpublished results). These data suggest that the GSG domain plays a dominant role in Sam68 localization but also requires the C terminus of Sam68 for proper localization.

Sam68:G→D and Sam68:I→N Associate with Microtubules

The fibrous pattern observed with Sam68:G→D and Sam68: I→N was characteristic of microtubules (Figure 5A, pattern E). To verify that these proteins were associated with microtubules, HeLa cells transfected with Sam68:G→D were immunostained with anti-tubulin antibodies and colocalization of Sam68 fibers with tubulin was analyzed with confocal microscopy. As shown in Figure 6A, some Sam68 fibers colocalized with tubulin. The tubulin staining was much weaker than the Sam68 staining, which may explain the partial colocalization with tubulin. To further confirm that the Sam68 fibers associated with microtubules, the effect of the microtubule-disrupting drug nocodazole on the integrity of these fibers was examined. Cells transfected with Sam68: G→D displaying a fibrous pattern were localized and photographed live before and after nocodazole treatment. After the addition of nocodazole for 15 and 30 min, the fibers completely disassembled (Figure 6B), suggesting that Sam68:G→D was associated with the microtubules or microtubule-associated proteins.

Characterization of the GFP-Sam68ΔL1 Nuclear Bodies

We wanted to verify that the nuclear bodies observed with GFP-Sam68ΔL1 and other Sam68 proteins harboring GSG

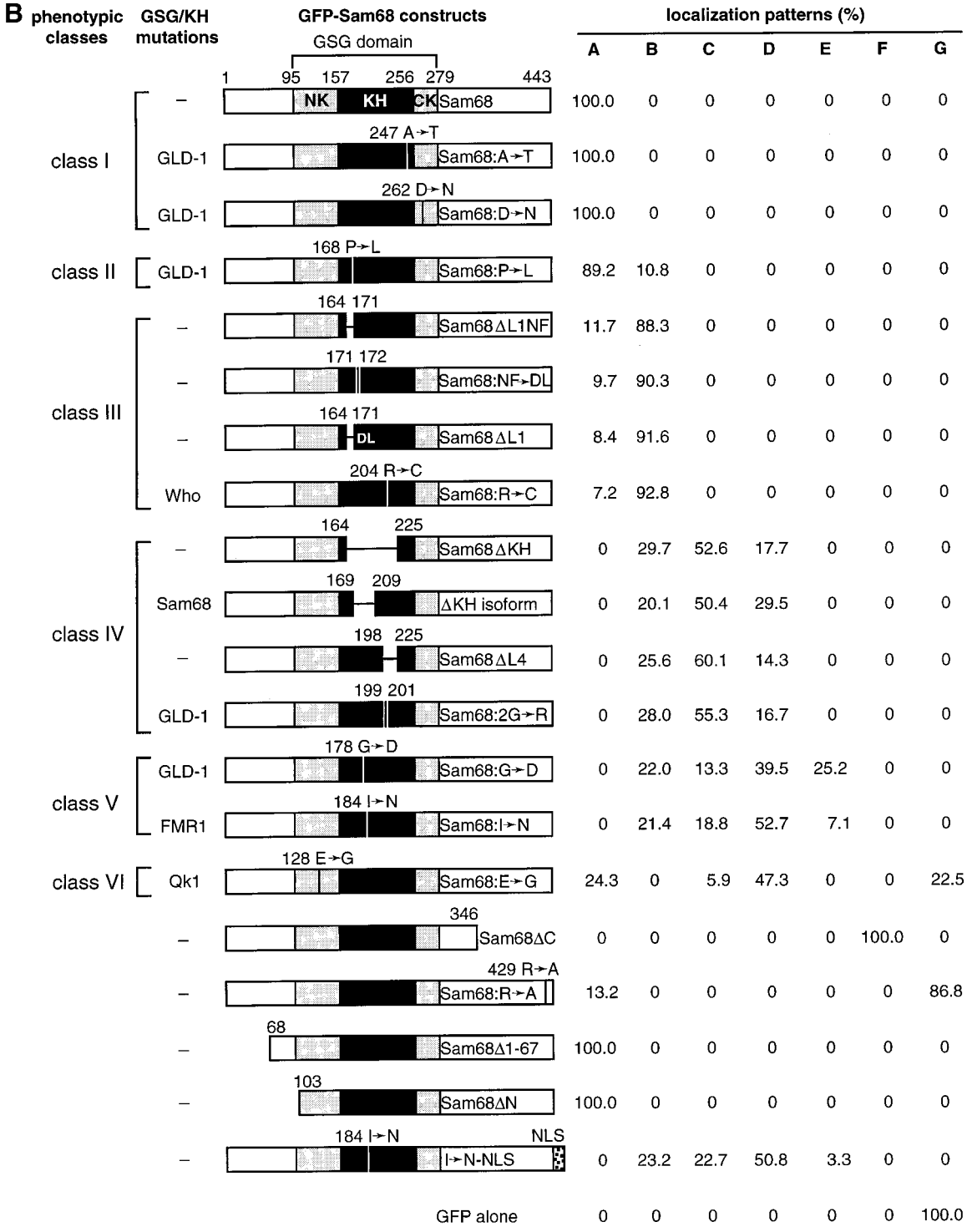

Figure 5 *continued.*

mutations/deletions behaved like endogenous SNBs. Initially, we examined whether the GFP-Sam68ΔL1 bodies were nuclear structures. Difference interference contrast microscopy of HeLa cells transfected with GFP-Sam68ΔL1 demonstrated that the nuclear bodies generated were bona fide nuclear structures (Figure 7A). The colocalization of GFP-Sam68ΔL1 nuclear bodies with other nuclear bodies was examined. Confocal microscopy revealed that GFP-

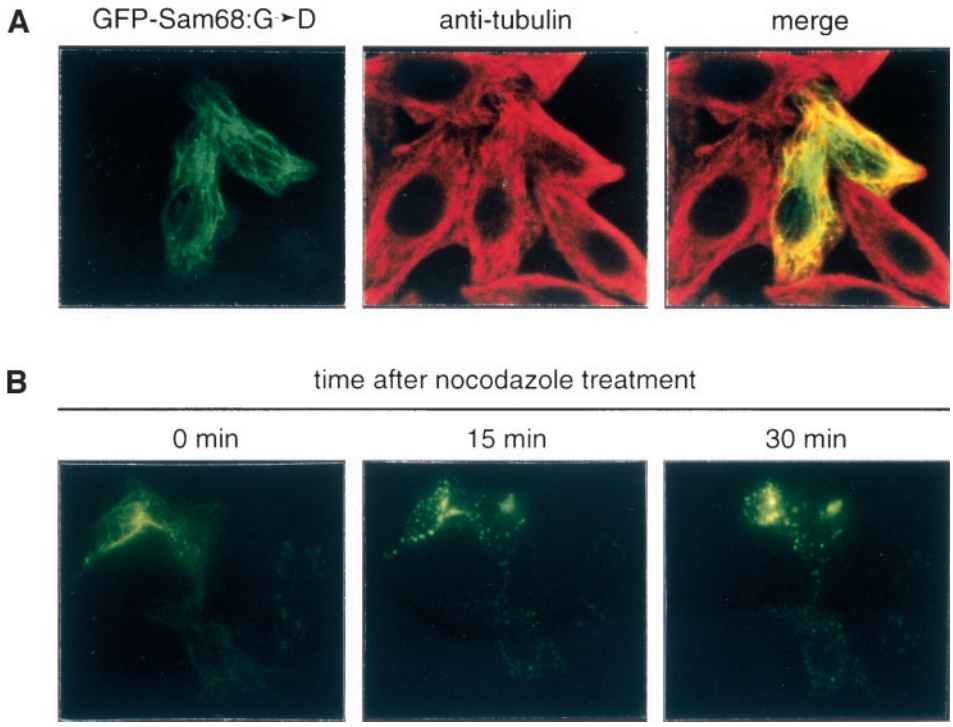

Figure 6. Sam68:G→D and Sam68:I→N associate with microtubules. (A) HeLa cells transfected with GFP-Sam68:G→D were fixed, permeabilized, and immunostained with anti-tubulin antibody followed by a rhodamine-conjugated goat anti-mouse secondary antibody and then analyzed by confocal microscopy. Colocalization of Sam68 fibers (green) with microtubule fibers (red) resulted in yellow color when the confocal images of GFP-Sam68:G→D and anti-tubulin immunostaining were merged. (B) HeLa cells transfected with GFP-Sam68:G→D were incubated with 40 ng/ml nocodazole, and cells with fibrous phenotype were photographed live before (0 min) and 15 or 30 min after the addition of nocodazole.

Sam68ΔL1 nuclear bodies did not colocalize with coiled bodies, gems, PML nuclear bodies, BCL6/SMRT nuclear structures, and fibrillarin, nor did they cause any of these structures to reorganize (our unpublished results).

The dynamics of the GFP-Sam68ΔL1 nuclear bodies were examined. As has been shown with endogenous SNBs, the GFP-Sam68ΔL1 nuclear bodies disassembled with actinomycin D treatment (Figure 7B). Coiled bodies and gems have been shown to increase in size at lower temperatures (Carmo-Fonseca *et al.*, 1993; Liu and Dreyfuss, 1996). HeLa cells transfected with GFP-Sam68ΔL1 were incubated at 32°C, and the nuclear bodies were clearly larger in size (Figure 7B), suggesting that GFP-Sam68ΔL1 nuclear bodies behaved like other nuclear bodies, such as coiled bodies and gems. It is interesting to note that proteins such as GFP-Sam68ΔL1 that gave a Sam68-exclusive nuclear body pattern were not expressed diffusely in the nucleoplasm 12–18 h after transfection. To further characterize the dynamic nature of GFP-Sam68ΔL1 nuclear bodies, cells transfected with GFP-Sam68ΔL1 were examined for 60 h (Figure 7C). At 12 h after transfection, GFP-Sam68ΔL1–transfected cells contained ~30 GFP-Sam68ΔL1 nuclear bodies. The size of these nuclear bodies increased with time, whereas the number decreased to <20 at 24–36 h after transfection. At 48–60 h, the GFP-Sam68ΔL1 nuclear bodies gradually disappeared and the nuclei displayed a diffuse extranucleolar staining, as was observed with wild-type Sam68 (Figure 7C). These findings further suggested that there exists a Sam68 equilibrium between SNBs and the nucleoplasm. This equilibrium is shifted in favor of the SNBs when Sam68 has certain amino acid substitutions or deletions in the GSG domain. Taken together, these data demonstrate that Sam68ΔL1 nuclear bodies share identical properties with endogenous SNBs.

SNBs Do Not Contain Nascent RNAs and snRNPs

To determine whether SNBs are involved in transcription, we performed in situ Br-UTP incorporation experiments (Figure 8A). HeLa cells transfected with GFP-Sam68 (Figure 8A, a–c), GFP-Sam68ΔL1 (Figure 8A, d–f), or GFP-PTB (Figure 8A, g–i) were briefly permeabilized and incubated in a transcription mixture containing Br-UTP. Then, the cells were fixed and the sites of transcription were detected by immunolabeling with a mAb that recognizes Br-UTP followed by a rhodamine-conjugated goat anti-mouse secondary antibody. Confocal microscopy revealed that both wild-type Sam68 and Sam68ΔL1 nuclear bodies did not colocalize with the major sites of Br-UTP incorporation (Figure 8A, a–c and d–f). As a positive control, we used GFP-PTB, which has been shown to colocalize in the perinucleolar compartment with newly synthesized RNA (Huang *et al.*, 1998). As expected, GFP-PTB colocalized with sites of Br-UTP incorporation (Figure 8A, g–i; colocalization indicated by arrows in i). The specificity of the Br-UTP incorporation assay was demonstrated by the fact that treatment of cells with actinomycin D prevented Br-UTP incorporation (our unpublished results). These findings indicate that SNBs do not represent major sites of transcription.

Coiled bodies have been found to contain spliceosomal snRNPs (Carmo-Fonseca *et al.*, 1993). Although gems do not contain snRNPs (Liu and Dreyfuss, 1996), as observed with immunofluorescence with the anti-Sm antibody Y12 (Petterson *et al.*, 1984), SMN has been shown to interact directly with Sm core proteins (Liu *et al.*, 1997). Moreover, a truncation of the N-terminal 27 amino acids of SMN causes the reorganization of snRNPs in the nucleus (Pellizzoni *et al.*, 1998). To determine whether SNBs contain splicing factors,

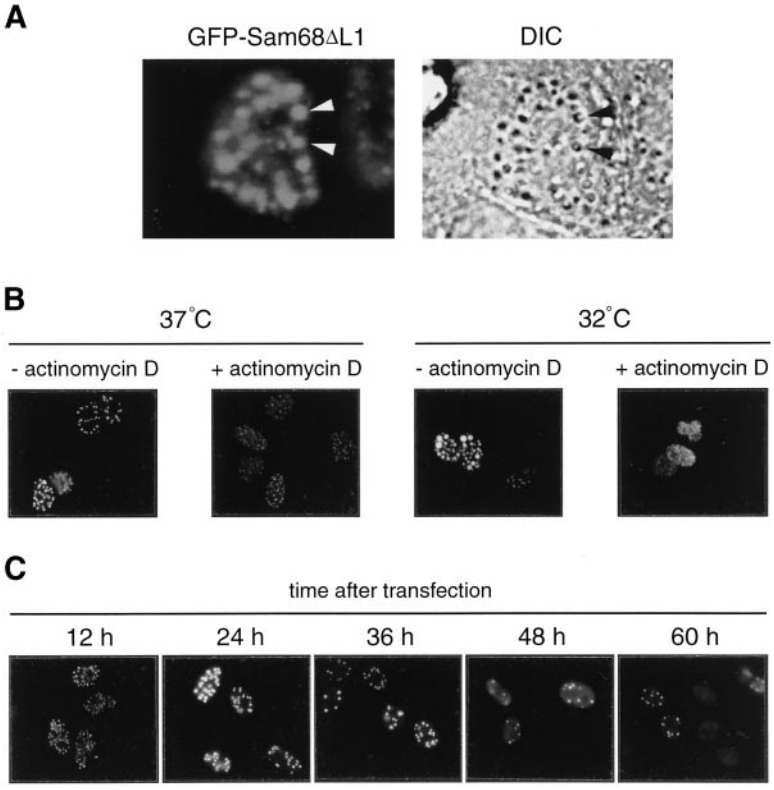

Figure 7. Characterization of GFP-Sam68ΔL1 nuclear bodies. (A) HeLa cells transfected with GFP-Sam68ΔL1 were fixed and analyzed with fluorescence and difference interference contrast (DIC) microscopy. (B) GFP-Sam68ΔL1 nuclear bodies are dynamic structures. HeLa cells were transfected with GFP-Sam68ΔL1 and then incubated at 37 or 32°C for 24 h; the last 3 h of incubation was performed with or without 5 μg/ml actinomycin D. The cells were fixed and visualized by fluorescence microscopy. (C) HeLa cells transfected with GFP-Sam68ΔL1 were fixed and observed 12, 24, 36, 48, or 60 h after transfection.

HeLa cells were double immunostained with anti-Sam68 AD1 (Figure 8Ba) and anti-SC35 antibodies (Figure 8Bb). The merged confocal image revealed that SNBs did not colocalize with SC35 (Figure 8Bc). HeLa cells expressing GFP-Sam68ΔL1 were also immunostained with the anti-SC35 and analyzed by confocal microscopy (Figure 8B, d–f). The Sam68ΔL1 nuclear bodies did not colocalize with SC35, although a few bodies seemed to partially overlap with SC35 (Figure 8B; indicated by arrows in f), which we suspect represent random overlapping because of the numerous bodies in both fields (Figure 8Bf). Moreover, both wild-type Sam68 and Sam68ΔL1 nuclear bodies were not stained with the anti-Sm antibody Y12 (our unpublished results). Taken together, these findings suggest that SNBs do not contain snRNPs. In addition, overexpression of Sam68ΔL1 did not change the pattern of anti-SC35 (Figure 8B; compare b and e), anti-coilin, and anti-SMN (our unpublished results) immunostaining. These findings suggest that Sam68ΔL1, in spite of inducing more SNBs, has no effect on the distribution and organization of coiled bodies, gems, and snRNPs.

Structure of the Sam68/SLM Nuclear Bodies by Correlative Microscopy

We used the technique of electron spectroscopic imaging to map protein-based and nucleic acid–based regions in and around SNBs. This technique allows comparison of nitrogen and phosphorus maps, providing the ability to directly distinguish protein from nucleic acids in situ based on elemental composition, without specific stains or labels (Hendzel *et al.*, 1999). To identify the nuclear bodies in the electron microscope images, we used a correlative fluorescence and electron microscopy approach. The sections of fluorescently labeled cells were first imaged in the fluorescence microscope to identify the nuclear bodies. Subsequently, the same sections were imaged by electron spectroscopic imaging (Hendzel *et al.* 1999). We have found that Sam68 nuclear bodies are large, spherical or ovoidal structures of ~0.6 × 1 μm (Figure 9). The SNBs are enriched in phosphorus-rich and nitrogen-rich fibers and granules, indicating the presence of nucleic acids (Figure 9, Net P and Net N images). These data further suggest that Sam68/SLM structures are nuclear bodies and that these structures are enriched in nucleic acids that may represent RNA.

DISCUSSION

We demonstrate that endogenous Sam68 localizes into novel nuclear structures that we have named SNBs for Sam68/SLM nuclear bodies. Alterations in the GSG domain resulted in several Sam68 cellular patterns, including exclusive SNB accumulation, microtubule association, diffuse cytoplasmic staining, and whole cell and cytoplasmic punctate staining. These observations implicate the Sam68 GSG domain in protein localization. The protein localization property was separate from the other GSG properties such as RNA binding and self-association, because Sam68 proteins defective in RNA binding (e.g., Sam68:G→D and Sam68:I→N; Chen *et al.*, 1997), self-association (e.g., Sam68ΔL1; Chen *et al.*, 1997), or both (e.g., Sam68ΔKH, Sam68ΔL4, and Sam68:2G→R;

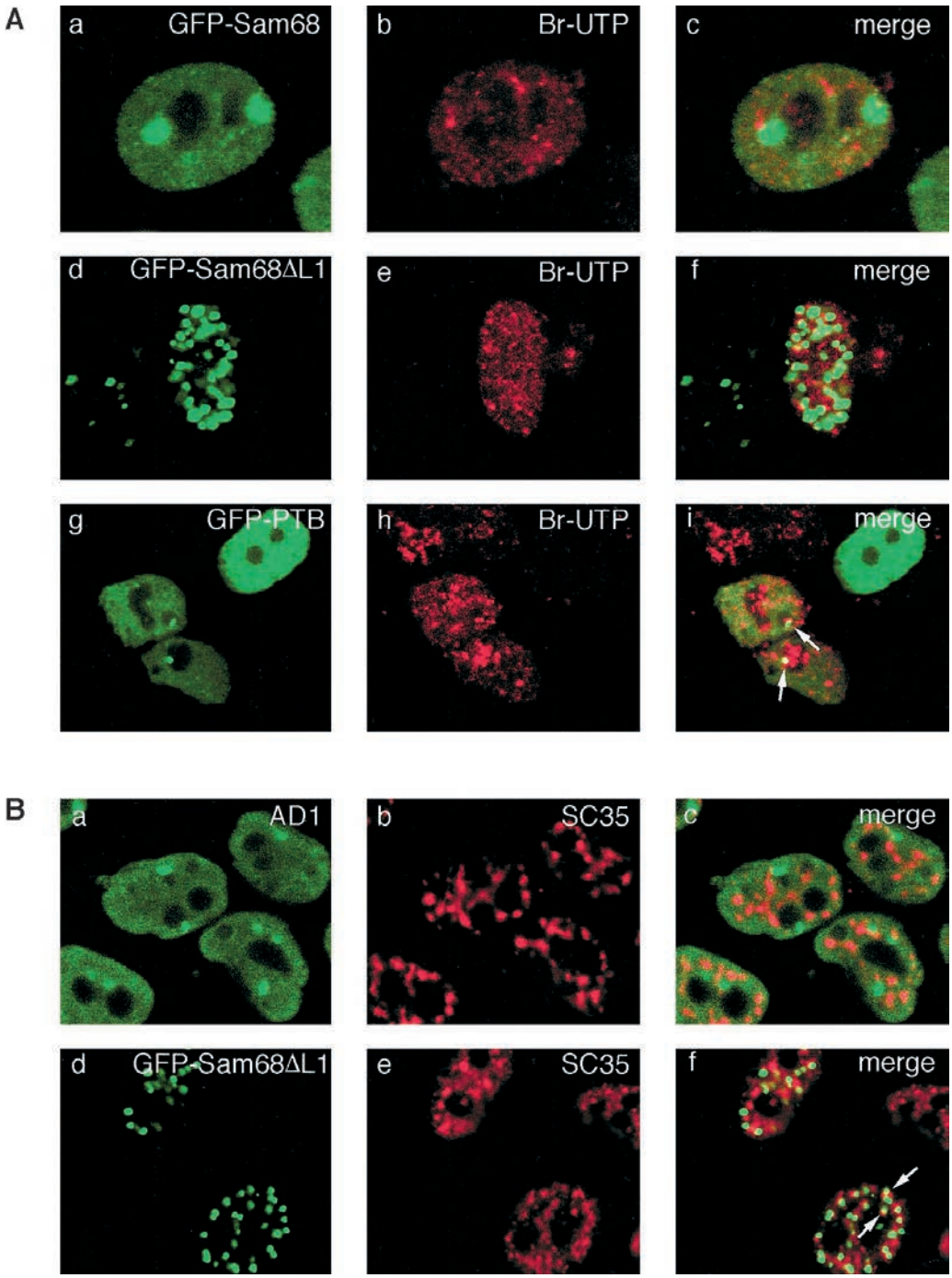

Figure 8. Sam68 nuclear bodies do not contain nascent RNAs and snRNPs. (A) HeLa cells transfected with GFP-Sam68 (a–c), GFP-Sam68ΔL1 (d–f), or GFP-PTB (g–i) were permeabilized with 50 μg/ml saponin for 5 min at 4°C and then incubated with a transcription cocktail containing Br-UTP for 20 min at 33°C. The cells were fixed, and the sites of Br-UTP incorporation were detected by immunolabeling using anti-BrdU antibody (which also recognizes Br-UTP) followed by a rhodamine-conjugated secondary antibody (b, e, and h). Colocalization was determined by confocal microscopy (c, f, and i). The arrows in panel i indicate colocalization of PNC with sites of Br-UTP incorporation. (B) HeLa cells (a–c) or HeLa cells transfected with GFP-Sam68ΔL1 (d–f) were fixed, permeabilized, and immunostained with anti-SC35 antibody followed by a secondary antibody conjugated to rhodamine (b and e). Endogenous Sam68 nuclear bodies were detected by immunolabeling using anti-Sam68 AD1 antibody followed by FITC-conjugated goat anti-rabbit antibody (a). Colocalization of SNBs and SC35 was analyzed by confocal microscopy (c and f). The arrows in panel f indicate partial overlap of Sam68ΔL1 SNBs with SC35, most likely random overlapping.

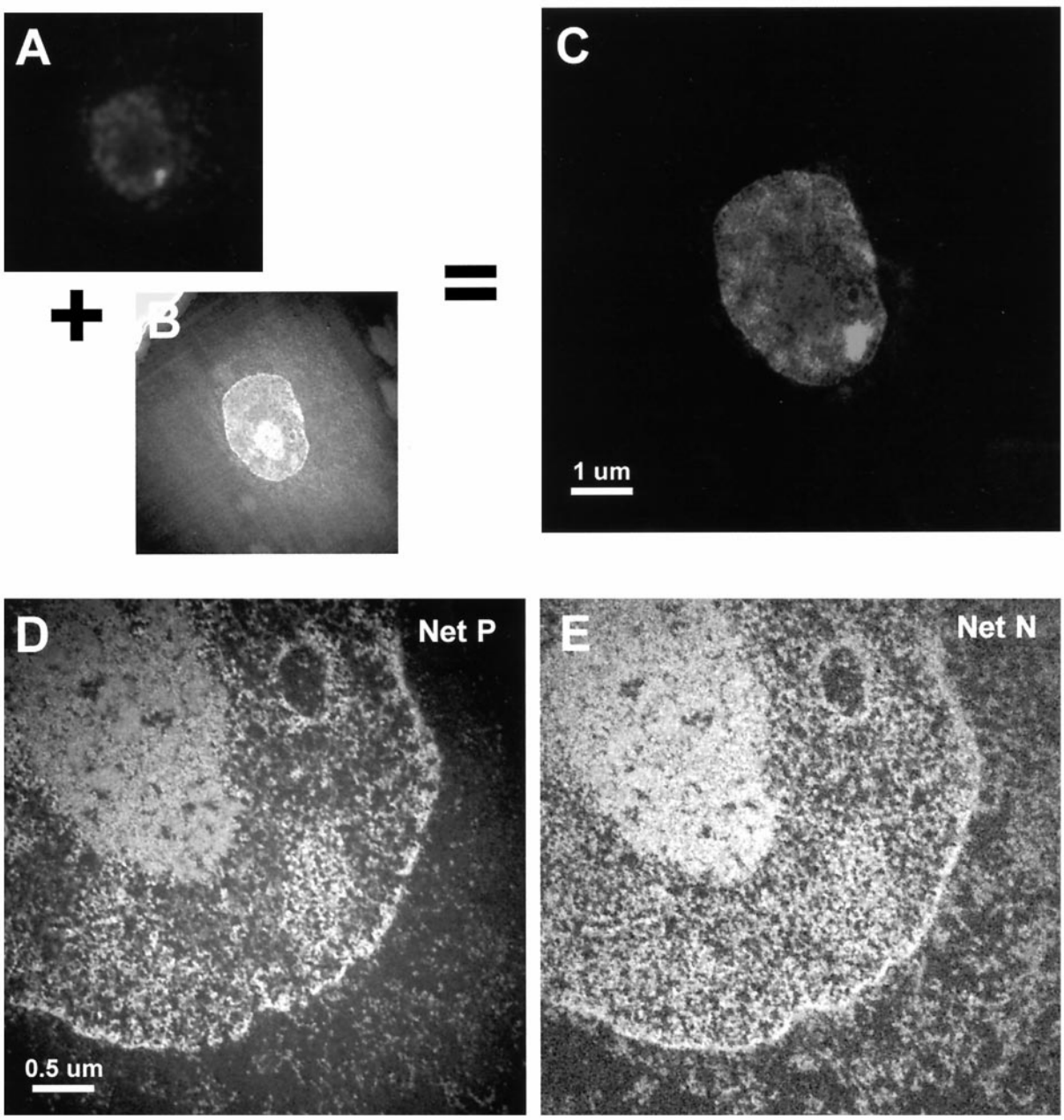

Figure 9. Correlative microscopy of Sam68 nuclear bodies. An ultrathin section (30 nm) of HeLa cells, previously labeled with anti-Sam68 AD1 antibody and embedded for electron microscopy, was examined under an immunofluorescence microscope (A) and then an electron microscope (B). The respective images were resized and rotationally aligned before being merged (C). It was then possible to identify the locations of structures labeled by immunofluorescence and to characterize them, by electron spectroscopic imaging, for phosphorus content (D) and nitrogen content (E). (Magnification: B and C, ×3,000; D and E, ×12,000).

Chen *et al.*, 1997) displayed altered localization. The localization property of the GSG domain is a bona fide role for this protein module. Thus, genetic mutations in the GSG domain can alter RNA binding, self-association, and/or the localization of a protein. The C-terminal tyrosine-rich region of Sam68 was required for proper Sam68 localization, suggesting that tyrosine phosphorylation of the C terminus of Sam68 may regulate its localization as it regulates RNA binding and self-association (Wang *et al.*, 1995; Chen *et al.*, 1997). Although RNA binding, self-association, and protein localization are separable properties of the GSG domain, they most likely function together to transport RNAs as protein multimers. Recently, Sam68 has been shown to function like HIV-1 Rev and may be its cellular homologue

(Reddy *et al.*, 1999). These findings are consistent with our data that Sam68 may be involved in transport of cellular RNAs.

It is not understood why mutations in the Sam68 GSG domain localize the mutant proteins to different cellular locations. The most likely explanation and the one we favor is that some Sam68 proteins containing amino acid substitutions or deletions are trapped in certain locations or "travel" slowly inside the cell. This allows these mutant Sam68 proteins to concentrate in areas where Sam68 would normally be found transiently. The patterns would then represent "snapshots" of the different journeys of Sam68 within the cell. It is also possible that the location of Sam68 mutants may be cell cycle regulated and may represent different locations of Sam68 during the cell cycle. The presence of Sam68 in both the cytoplasm and the nucleus suggests that it shuttles like other RNA-binding proteins, including hnRNP K and A1 (Pinol-Roma and Dreyfuss, 1992; Michael *et al.*, 1997). A high-affinity RNA-binding motif (UAAA), present in most if not all mRNAs, has been identified for Sam68 (Lin *et al.*, 1997). This information, coupled with the possibility that Sam68 shuttles between the nucleus and the cytoplasm, raises the question of whether Sam68 functions as a general transporter protein for RNAs. The presence of Sam68 in specialized nuclear structures suggests that Sam68 may also have a specialized function in RNA metabolism, such as snRNP biogenesis or pre-mRNA processing. The localization of Sam68 to microtubules also raises the possibility that Sam68 may be transiently associated with the mitotic spindle or that Sam68 bridges RNAs to microtubules or travels along the microtubules. A bridging function was recently shown for the *Xenopus* KH domain protein Vg1 RBP that bridges the Vg1 mRNA to microtubules (Havin *et al.*, 1998).

The expression of GFP-SLM-1 and GFP-SLM-2 in HeLa cells resulted in colocalization with Sam68 in SNBs, suggesting that SLM-1 and SLM-2 are also components of SNBs. Interestingly, unlike Sam68 and SLM-1, GFP-SLM-2 was also localized or even concentrated in the nucleoli of ~60% of the transfected HeLa cells. This raises the possibility that SLM-2 as well as SNBs may be involved in some aspects of nucleolar functioning, such as rRNA and ribosome biogenesis. The observation that SNBs are frequently found in close proximity to the nucleoli also supports this possibility.

The function of most nuclear bodies is still largely unknown. Many components have been identified in coiled bodies and gems to suggest that these nuclear structures function in some aspect of snRNP biogenesis or pre-mRNA processing (Lamond and Earnshaw, 1998). The absence of SC35 and Sm proteins in SNBs, as detected by immunofluorescence with anti-SC35 and the Y12 anti-Sm antibodies (our unpublished results), suggests that snRNPs are not present in SNBs. Because SMN has been shown to associate directly with Sm core proteins (Liu *et al.*, 1997), we performed coimmunoprecipitation experiments with individual Sm core proteins to further examine the possibility that Sm proteins associated with Sam68. No convincing association was observed between Sam68 and individually overexpressed Sm proteins, including HA epitope–tagged Sm-B, Sm-D1, Sm-D3, Sm-E, Sm-F, and Sm-G (our unpublished results). These Sm proteins are known to be the major protein components of the snRNPs (Mattaj and DeRobertis, 1985). Thus, we conclude that Sam68 does not associate directly with Sm core proteins and that SNBs, unlike coiled bodies, do not contain snRNPs.

SNBs are primarily present in cancer cells, suggesting that they may be linked to cell transformation. Either SNBs contribute to the transformed phenotype or they are a consequence of transformation. The fact that SNB prevalence varies significantly among transformed cells indicates that the presence of SNBs is cell type specific and/or may be related to the degree of malignancy. The latter possibility is supported by the observation that SNB prevalence correlated with the differentiation status and tumorigenicity of the three breast cancer cell lines examined. BT-20 cells, a poorly differentiated cell line that induces tumors in nude mice, has a much higher SNB prevalence (~90%) than Hs 578T cells (~50%), which are not tumorigenic in nude mice. On the other hand, MCF-7 cells, a well-differentiated cell line, had the lowest SNB prevalence, with ~5% of the cells containing SNBs. SNBs may be a useful marker for certain cancers.

The importance of nuclear bodies is highlighted by their linkage to certain diseases. The number of coiled bodies or PNCs is significantly increased in transformed cells (Spector *et al.*, 1992; Huang *et al.*, 1997). Gems contain SMN (Liu and Dreyfuss, 1996), the protein responsible for spinal muscular atrophy (Bussaglia *et al.*, 1995; Lefebvre *et al.*, 1995). PML nuclear bodies are disorganized in patients with acute promyelocytic leukemia (Dyck *et al.*, 1994; Weis *et al.*, 1994; Doucas *et al.*, 1996). *BRCA1* and *BRCA2*, known tumor-suppressor genes that account for most cases of familial, early-onset breast and/or ovarian cancer, localize into nuclear bodies (Miki *et al.*, 1994; Wooster *et al.*, 1995). The oncoprotein LAZ3/BCL6 and the corepressor SMRT have been shown to colocalize to nuclear bodies (Dhordain *et al.*, 1997). Disruption of the *LAZ3/BCL6* gene because of the chromosomal translocation 3q27 causes diffuse large cell lymphomas (Kerckaert *et al.*, 1993; Ye *et al.*, 1993). Intranuclear inclusions composed of mutant proteins have been found in cells affected by several neurodegenerative diseases, including Huntington's disease and type 1 spinocerebellar ataxia (Sisodia, 1998).

HeLa cells transfected with GFP-Sam68 have a diffuse nuclear staining with 2–5 SNBs. On the other hand, HeLa cells transfected with GFP-Sam68ΔL1 have 10–30 SNBs with no diffuse nuclear staining. Because the Sam68 GFP fusion proteins were expressed to similar levels, as detected by Western blotting (our unpublished results), this suggests that all of the GFP-Sam68ΔL1 concentrates in SNBs. The question that arises is whether new SNBs are created or existing undetectable SNBs increase in size and become visible. The fact that SNBs generated by GFP-Sam68ΔL1 relocalize to diffuse nuclear staining after 48–60 h suggests that SNBs are in equilibrium with the nucleoplasm. The labeling with Br-UTP demonstrates that SNBs are not the site of active transcription, as has been shown for the perinucleolar compartment (Huang *et al.*, 1998). However, SNBs do contain nucleic acids that may be RNA, as detected using correlative electron microscopy (Figure 9). Because we have shown that Sam68 oligomerization is RNA dependent (Chen *et al.*, 1997), it is possible that SNBs form only in cells that contain specific Sam68/SLM RNA targets.

Previous immunofluorescence studies on Sam68 did not reveal SNBs in NIH 3T3 cells (Ishidate *et al.*, 1997). Although

there are several factors that can influence the presence and detection of SNBs, such as the antibody, fixation, and cell type, we believe that the major reason in this study was the use of NIH 3T3 cells. We found that overexpression of GFP-Sam68 in NIH 3T3, REF-52, or COS cells does not result in the appearance of SNBs, consistent with the data reported by Ishidate *et al.* (1997). Another Sam68 immunofluorescence study using HeLa cells and NIH 3T3 cells did not detect SNBs (McBride *et al.*, 1998). In that study, the cells were fixed with methanol before staining with anti-Sam68 antibodies. We found that such a fixation procedure results in a granular nuclear staining pattern and made SNBs hard to detect (our unpublished results). Furthermore, McBride *et al.*, (1998) showed that Sam68 localized in punctate nuclear structures in HeLa cells upon treatment with transcription inhibitors. These data contradict our observations that transcription inhibitors, including actinomycin D and α-amanitin, disassemble SNBs. Because we show that SNBs disassemble with transcription inhibitors in several situations, including in live cells, we believe the difference is due to the fixation-permeabilization procedure. Recently, another study demonstrated that overexpression of T-STAR/ETOILE (human SLM-2) in HeLa cells, but not in COS cells, resulted in nuclear bodies similar to SNBs (Venables *et al.*, 1999). These nuclear structures did not colocalize with coiled bodies, the PNC, and Y12-stained structures (Venables *et al.*, 1999), consistent with our observations. We have observed that not all nuclear GSG proteins localize in SNBs in HeLa cells (our unpublished results); thus, SNBs may not be a general site for all nuclear GSG proteins.

In conclusion, we have identified a novel nuclear structure that contains Sam68, SLM-1, and SLM-2. We have termed these structures Sam68/SLM nuclear bodies. SNBs are dynamic structures primarily present in cancer cells that are distinct from coiled bodies, gems, and PML nuclear bodies. Alterations in the GSG domain of Sam68 gave six separate classes of Sam68 cellular patterns, including exclusive SNB localization and association with the microtubules. Our data imply that the GSG domain is a multifunctional protein module involved in protein localization and define a new cellular compartment in transformed cells for Sam68/SLM proteins.

ACKNOWLEDGMENTS

We thank Hugo Dilhuydy at the Centre de Recherche Institut Universitaire de Gériatrie de Montréal for excellent help and assistance with the confocal microscopy. We thank Manfred Herfort for excellent technical assistance and Mark Bedford for the SmB antibodies, for critically reading the manuscript, and for helpful discussions. We thank Edward Chan for the anti-coilin antibodies, Michael Pollard for the anti-fibrillarin antibodies, and Yuri Svitkin and Nahum Sonenberg for the PTB cDNA. We are grateful to members of the Wilson Miller lab for helpful discussions. This work was supported by research grants from the Medical Research Council of Canada and the Cancer Research Society to S.R. and D.P.B.-J. T.C. is a recipient of the Doctoral Research Award from the Medical Research Council of Canada, and S.R. is a scholar of the Medical Research Council of Canada.

REFERENCES

Andrade, L.E.C., Tan, E.M., and Chan, E.K.L. (1993). Immunocytochemical analysis of the coiled body in the cell cycle and during cell proliferation. Proc. Natl. Acad. Sci. USA *90*, 1947–1951.

Arning, S., Gruter, P., Bilbe, G., and Kramer, A. (1996). Mammalian splicing factor SF1 is encoded by variant cDNAs and binds to RNA. RNA *2*, 794–810.

Baehrecke, E.H. (1997). who encodes a KH RNA binding protein that functions in muscle development. Development *124*, 1323–1332.

Barlat, I., Maurier, F., Duchesne, M., Guitard, E., Tocque, B., and Schweighoffer, F. (1997). A role for Sam68 in cell cycle progression antagonized by a spliced variant within the KH domain. J. Biol. Chem. *272*, 3129–3132.

Bazett-Jones, D.P., and Hendzel, M.J. (1999). Electron spectroscopic imaging of chromatin. Methods *17*, 188–200.

Bechade, C., Rostaing, P., Cisterni, C., Kalusch, R., La Bella, V., Pettmann, B., and Triller, A. (1999). Subcellular distribution of survival motor neuron (SMN) protein: possible involvement in nucleocytoplasmic and dendritic transport. Eur. J. Neurosci. *11*, 293–304.

Berglund, J.A., Chua, K., Abovich, N., Reed, R., and Rosbash, M. (1997). The splicing factor BBP interacts specifically with the pre-mRNA branch-point sequence UACUAAC. Cell *89*, 781–787.

Bussaglia, E., Clermont, O., Tizzano, E., Lefebvre, S., Burglen, L., Cruaud, C., and Urtizberea, J.A. (1995). A frame-shift deletion in the survival motor neuron gene in Spanish spinal muscular atrophy patients. Nat. Genet. *11*, 335–337.

Carmo-Fonseca, M., Ferreira, J., and Lamond, A.I. (1993). Assembly of snRNP-containing coiled bodies is regulated in interphase and mitosis: evidence that the coiled body is a kinetic nuclear structure. J. Cell Biol. *120*, 841–852.

Chen, T., Damaj, B., Herrerra, C., Lasko, P., and Richard, S. (1997). Self-association of the single-KH domain family members Sam68, GRP33, GLD-1 and Qk1: role of the KH domain. Mol. Cell. Biol. *17*, 5707–5718.

Chen, T., and Richard, S. (1998). Structure-function analysis of Qk1: a lethal point mutation in mouse quaking prevents homodimerization. Mol. Cell. Biol. *18*, 4863–4871.

Cruz-Alvarez, M., and Pellicer, A. (1987). Cloning of a full-length complementary DNA for an *Artemia salina* glycine-rich protein. J. Biol. Chem. *262*, 13377–13380.

DeBoulle, K., Verkerk, A.J.M.H., Reyniers, E., Vits, L., Hendrickx, J., Roy, B.V., Bos, F.V.D., DeGraaff, E., Oostra, B.A., and Willems, P.J. (1993). A point mutation in the FMR-1 gene associated with fragile X mental retardation. Nat. Genet. *3*, 31–35.

Dhordain, P., Albagli, O., Lin, R.J., Ansieau, S., Quief, S., Leutz, A., Kerckaert, J.P., Evans, R.M., and Leprince, D. (1997). Corepressor SMRT binds the BTB/POZ repressing domain of the LAZ3/BCL6 oncoprotein. Proc. Natl. Acad. Sci. USA *94*, 10762–10767.

Di Fruscio, M., Chen, T., Bonyadi, S., Lasko, P., and Richard, S. (1998). The identification of two *Drosophila* KH domain proteins: KEP1 and SAM are members of the Sam68 family of GSG domain proteins. J. Biol. Chem. *273*, 30122–30130.

Di Fruscio, M., Chen, T., and Richard, S. (1999). Two novel Sam68-like mammalian proteins SLM-1 and SLM-2: SLM-1 is a Src substrate during mitosis. Proc. Natl. Acad. Sci. USA *96*, 2710–2715.

Doucas, V., Ishov, A.M., Romo, A., Juguilon, H., Weitzman, M.D., Evans, R.M., and Maul, G.G. (1996). Adenovirus replication is coupled with the dynamic properties of the PML nuclear structure. Genes Dev. *10*, 196–207.

Dyck, J.A., Maul, G.G., Miller, W.H., Chen, J.D., Kakizuka, A., and Evans, R.M. (1994). A novel macromolecular structure is a target of

the promyelocyte-retinoic acid receptor oncoprotein. Cell *76*, 333–343.

Ebersole, T.A., Chen, Q., Justice, M.J., and Artzt, K. (1996). The *quaking* gene unites signal transduction and RNA binding in the developing nervous system. Nat. Genet. *12*, 260–265.

Feng, Y., Absher, D., Eberhart, D.E., Brown, V., Malter, H.E., and Warren, S.T. (1997). FMRP associates with polyribosomes as an mRNP, and the I304N mutation of severe fragile X syndrome abolishes this association. Mol. Cell *1*, 109–118.

Fischer, U., Liu, Q., and Dreyfuss, G. (1997). The SMN-SIP1 complex has an essential role in spliceosomal snRNP biogenesis. Cell *90*, 1023–1029.

Francis, R., Barton, M.K., Kimbel, J., and Schedl, T. (1995a). Control of oogenesis, germline proliferation and sex determination by the *C. elegans* gene gld-1. Genetics *139*, 579–606.

Francis, R., Maine, E., and Schedl, T. (1995b). Gld-1 a cell-type specific tumor suppressor gene in *C. elegans*. Genetics *139*, 607–630.

Fu, X.D., and Maniatis, T. (1990). Factor required for mammalian spliceosome assembly is localized to discrete regions in the nucleus. Nature *343*, 437–441.

Fumagalli, S., Totty, N.F., Hsuan, J.J., and Courtneidge, S.A. (1994). A target for Src in mitosis. Nature *368*, 871–874.

Fyrberg, C., Becker, J., Barthmaier, P., Mahaffey, J., and Fyrberg, E. (1997). A *Drosophila* muscle-specific gene related to the mouse quaking locus. Gene *197*, 315–323.

Fyrberg, C., Becker, J., Barthmaier, P., Mahaffey, J., and Fyrberg, E. (1998). A family of *Drosophila* genes encoding quaking-related Maxi-KH domains. Biochem. Genet. *36*, 51–64.

Gall, J.G., Tsvetkov, A., Wu, Z.A., and Murphy, C. (1995). Is the sphere organelle/coiled body a universal nuclear component? Dev. Genet. *16*, 25–35.

Gibson, T.J., Thompson, J.D., and Heringa, J. (1993). The KH domain occurs in a diverse set of RNA-binding proteins that include the antiterminator NusA and is probably involved in binding to nucleic acid. FEBS Lett. *324*, 361–366.

Havin, L., Git, A., Elisha, Z., Oberman, F., Yaniv, K., Schwartz, S.P., Standart, N., and Yisraeli, J.K. (1998). RNA-binding protein conserved in both microtubule- and microfilament-based RNA localization. Genes Dev. *12*, 1593–1598.

Hendzel, M.J., Boisvert, F.-M., and Bazett-Jones, D.P. (1999). Direct visualization of a protein nuclear architecture. Mol. Biol. Cell *10*, 2051–2062.

Hogan, E.L, and Greenfield, S. (1984). Animal models of genetic disorders of myelin. In: Myelin, 2nd ed., ed. P. Morrell, New York: Plenum Press, 489–534.

Huang, S., Deerinck, T.J., Ellisman, M.H., and Spector, D.L. (1997). The dynamic organization of the perinucleolar compartment in the cell nucleus. J. Cell Biol. *137*, 965–974.

Huang, S., Deerinck, T.J., Ellisman, M.H., and Spector, D.L. (1998). The perinucleolar compartment and transcription. J. Cell Biol. *143*, 35–47.

Ishidate, T., Yoshihara, S., Kawasaki, Y., Roy, B.C., Toyoshima, K., and Akiyama, T. (1997). Identification of a novel nuclear localization signal in Sam68. FEBS Lett. *409*, 237–241.

Jackson, D., Hassan A.B., Errington R.J., and Cook P.R. (1993). Visualization of focal sites of transcription within human nuclei. EMBO J. *12*, 1059–1065.

Jones, A.R., and Schedl, T. (1995). Mutations in GLD-1, a female germ cell-specific tumor suppressor gene in *C. elegans*, affect a conserved domain also found in Sam68. Genes Dev. *9*, 1491–1504.

Justice, M.J., and Bode, V.C. (1988). Three ENU-induced alleles of the murine quaking locus are recessive embryonic lethal mutations. Genet. Res. *51*, 95–102.

Kalderon, D., Roberts, B.L., Richardson, W.D., and Smith, A.E. (1984). A short amino acid sequence able to specify nuclear location. Cell *39*, 499–509.

Kerckaert, J.P., Deweindt, C., Tilly, H., Quief, S., Lecocq, G., and Bastard, C. (1993). LAZ3, a novel zinc-finger encoding gene, is disrupted by recurring chromosome 3q27 translocations in human lymphomas. Nat. Genet. *5*, 66–70.

Koken, M.H.M., *et al.* (1994). The t(15;17) translocation alters a nuclear body in a retinoic acid-reversible fashion. EMBO J. *13*, 1073–1083.

Lamond, A.I., and Carmo-Fonseca, M. (1993). The coiled body. Trends Cell Biol. *3*, 198–204.

Lamond, A.I., and Earnshaw, W.C. (1998). Structure and function in the nucleus. Science *280*, 547–553.

Lefebvre, S., *et al.* (1995). Identification and characterization of a spinal muscular atrophy-determining gene. Cell *89*, 155–165.

Lin, Q., Taylor, S.J., and Shalloway, D. (1997). Specificity and determinants of Sam68 RNA binding. J. Biol. Chem. *272*, 27274–27280.

Liu, Q., and Dreyfuss, G. (1996). A novel nuclear structure containing the survival of motor neurons protein. EMBO J. *15*, 3555–3565.

Liu, Q., Fischer, U., Wang, F., and Dreyfuss, G. (1997). The spinal muscular atrophy gene product, SMN, and its associated protein SIP1 are in a complex with spliceosomal snRNP proteins. Cell *90*, 1013–1021.

Matera, A.G., and Frey, M.R. (1998). Coiled bodies and gems: janus or gemini? Am. J. Hum. Genet. *63*, 317–321.

Mattaj, I.W., and DeRobertis, E.M. (1985). Nuclear segregation of U2 snRNA requires binding of specific snRNP proteins. Cell *40*, 111–118.

McBride, A.E., Taylor, S.J., Shalloway, D., and Kirkegaad, K. (1998). KH domain integrity is required for wild-type localization of Sam68. Exp. Cell Res. *241*, 84–95.

Michael, W.M., Eder, P.S., and Dreyfuss, G. (1997). The K nuclear shuttling domain: a novel signal for nuclear import and nuclear export in the hnRNP K protein. EMBO J. *16*, 3587–3598.

Miki, Y., *et al.* (1994). A strong candidate for the breast and ovarian cancer susceptibility gene BRCA1. Science *266*, 66–71.

Monneron, A., and Bernhard, W. (1969). Fine structural organization of the interphase nucleus in some mammalian cells. J. Ultrastruct. Res. *27*, 266–288.

Musco, G., Stier, G., Joseph, C., Morelli, M.A., and Pastore, A. (1996). Three-dimensional structure and stability of the KH domain: molecular insights into the fragile X syndrome. Cell *85*, 237–245.

Patton, J., Mayer, S.A., Tempst, P., and Nadal-Ginard, B. (1991). Characterization and molecular cloning of polypyrimidine tract-binding protein: a component of a complex necessary for pre-mRNA splicing. Genes Dev. *5*, 1237–1251.

Pellizzoni, L., Kataoka, N., Charroux, B., and Dreyfuss, G. (1998). A novel function for SMN, the spinal muscular atrophy disease gene product, in pre-mRNA splicing. Cell *95*, 615–624.

Petterson, I., Hinterberger, M., Mimori, T., Gottlieb, E., and Steitz, J. A. (1984). The structure of mammalian small nuclear ribonucleoproteins: identification of multiple protein components reactive with anti-(U1) ribonucleoprotein and anti-Sm autoantibodies. J. Biol. Chem. *259*, 5907–5914.

Pinol-Roma, S., and Dreyfuss, G. (1992). Shuttling of pre-mRNA binding proteins between nucleus and cytoplasm. Nature *355*, 730–732.

Pombo, A., Cuello, P., Schul, W., Yoon, J.B., Roeder, R.G., Cook, P.R., and Murphy, S. (1998). Regional and temporal specialization in the nucleus: a transcriptionally-active nuclear domain rich in PTF, Oct1 and PIKA antigens associates with specific chromosomes early in the cell cycle. EMBO J. *17*, 1768–1778.

Rain, J.C., Rafi, Z., Rhani, Z., Legrain, P., and Kramer, A. (1998). Conservation of functional domains involved in RNA binding and protein-protein interactions in human and *Saccharomyces cerevisiae* pre-mRNA splicing factor SF1. RNA *4*, 551–565.

Reddy, T.R., Xu, W., Mau, J.K.L., Goodwin, C.D., Suhasini, M., Tang, H., Frimpong, K., Rose, D.W., and Wong-Staal, F. (1999). Inhibition of HIV replication by dominant negative mutants of Sam68, a functional homolog of HIV-1 Rev. Nat. Med. *5*, 635–642.

Richard, S., Yu, D., Blumer, K.J., Hausladen, D., Olszowy, M.W., Connelly, P.A., and Shaw, A.S. (1995). Association of p62, a multifunctional SH2- and SH3-binding protein, with src-family tyrosine kinases, Grb2, and phospholipase Cγ-1. Mol. Cell. Biol. *15*, 186–197.

Siomi, H., Choi, M., Siomi, M.C., Nussbaum, R.L., and Dreyfuss, G. (1994). Essential role for KH domain in RNA binding: impaired RNA binding by a mutation in the KH domain of FMR1 that causes fragile X syndrome. Cell *77*, 33–39.

Sisodia, S.S. (1998). Nuclear inclusions in glutamine repeat disorders: are they pernicious, coincidental, or beneficial? Cell *95*, 1–4.

Spector, D.L. (1993). Nuclear organization of pre-mRNA processing. Curr. Opin. Cell Biol. *5*, 442–447.

Spector, D.L., Lark, G., and Huang, S. (1992). Differences in snRNP localization between transformed and nontransformed cells. Mol. Biol. Cell *3*, 555–569.

Tanaka, H., Abe, K., and Kim, C.H. (1997). Cloning and expression of the quaking gene in the zebrafish embryo. Mech. Dev. *69*, 209–213.

Taylor, S.J., Anafi, M., Pawson, T., and Shalloway, D. (1995). Functional interaction between c-src and its mitotic target, Sam68. J. Biol. Chem. *270*, 10120–10124.

Taylor, S.J., and Shalloway, D. (1994). An RNA-binding protein associated with src through its SH2 and SH3 domains in mitosis. Nature *368*, 867–871.

Venables, J.P., Vernet, C., Chew, S.L., Elliot, D.J., Cowmeadow, R.B., Wu, J., Cooke, H.J., Artzt, K., and Eperon, I.C. (1999). T-STAR/ETOILE: a novel relative of Sam68 that interacts with an RNA-binding protein implicated in spermatogenesis. Hum. Mol. Genet. *8*, 959–969.

Vernet, C., and Artzt, K. (1997). STAR, a gene family involved in signal transduction and activation of RNA. Trends Genet. *13*, 479–484.

Wang, L.L., Richard, S., and Shaw, A.S. (1995). p62 association with RNA is regulated by tyrosine phosphorylation. J. Biol. Chem. *270*, 2010–2013.

Weis, K., Rambaud, S., Lavau, C., Jansen, J., Carvalho, T., Carmo-Fonseca, M., Lamond, A., and Dejean, A. (1994). Retinoic acid regulates aberrant nuclear localization of PML-RARa in acute promyelocytic leukemia cells. Cell *76*, 345–356.

Willems, M., Penman, M., and Penmen, S. (1969). The regulation of RNA synthesis and processing in the nucleolus during inhibition of protein synthesis. J. Cell Biol. *41*, 177–187.

Wong, G., Muller, O., Clark, R., Conroy, L., Moran, M.F., Polakis, P., and McCormick, F. (1992). Molecular cloning and nucleic acid binding properties of the GAP-associated tyrosine phosphoprotein p62. Cell *69*, 551–558.

Wooster, R., *et al.* (1995). Identification of the breast cancer susceptibility gene BRCA2. Nature *378*, 789–792.

Ye, B.H., Lista, F., Lo Coco, F., Knowles, D.M., Offit, K., Chaganti, R.S.K., and Dalla-Favera, R. (1993). Alterations of a zinc finger-encoding gene, BCL-6, in diffuse large-cell lymphoma. Science *262*, 747–750.

Zaffran, S., Astier, M., Gratecos, D., and Semeriva, M. (1997). The held out wings (how) *Drosophila* gene encodes a putative RNA binding protein involved in the control of muscular and cardiac activity. Development *124*, 2087–2098.

Zorn, A.M., Grow, M., Patterson, K.D., Ebersole, T.A., Chen, Q., Artzt, K., and Krieg, P.A. (1997). Remarkable sequence conservation of transcripts encoding amphibian and mammalian homologues of *quaking*, a KH domain RNA-binding protein. Gene *188*, 199–206.

Zorn, A.M., and Krieg, P.A. (1997). The KH domain protein encoded by quaking functions as a dimer and is essential for notochord development in *Xenopus* embryos. Genes Dev. *11*, 2176–2190.